1-1-2011

Self-shape optimisation of cold-formed steel closed profiles using genetic algorithms

Benoit Gilbert
Griffith University, b.gilbert@griffith.edu.au

Lip H. Teh
University of Wollongong, lteh@uow.edu.au

Hong Guan
Griffith University, h.guan@griffith.edu.au

Self-shape optimisation of cold-formed steel closed profiles using genetic algorithms

Abstract

For economical benefits, optimisation of mass-produced structural steel products is widely researched. The objective is to minimise the quantity of material used without sacrificing the strength and practicality of the structural members. Current research focuses on optimising the dimensions of conventional cross-sectional shapes but rarely considers discovering new optimum shapes. This report introduces the concepts of a new optimisation method which enables the crosssection to self-shape to an optimum by using the evolution and adaptation benefits of Genetic Algorithm. The feasibility and accuracy of the method are verified by implementing it to find optimum thin-walled profiles against simple parameters for which analytical solutions are known, namely the optimisation of doubly-symmetric closed profiles. Results show that the cross-section accurately self-shapes to its optimum in a low number of generations. Factors influencing the convergence are presented and future challenges to applying the method to optimisation of cold-formed steel profiles with practical applications are discussed.

Keywords

closed, steel, formed, genetic, cold, profiles, algorithms, optimisation, shape, self

Disciplines

Engineering | Science and Technology Studies

Publication Details

Gilbert, B., Teh, L. H. & Guan, H. (2011). Self-shape optimisation of cold-formed steel closed profiles using genetic algorithms. 6th International Conference on Thin Walled Structures (pp. 595-602). Qld, Australia: Griffith University.

CENTRE FOR INFRASTRUCTURE ENGINEERING AND MANAGEMENT

SELF-SHAPE OPTIMISATION OF COLD-FORMED STEEL CLOSED PROFILES USING GENETIC ALGORITHM

Research report CIEM/2011/R01

BENOIT P. GILBERT
LIP H. TEH
HONG GUAN

February 2011
ISSN 1839-292X

ISSN 1839-292X

Published by:
Centre for Infrastructure Engineering and Management
Griffith University QLD 4222
Australia

This report and other Research Reports published by the Centre for Infrastructure Engineering and Management are available at http://www.griffith.edu.au/engineering-information-technology/centre-infrastructure-engineering-management/publications/technical-reports

ABSTRACT

For economical benefits, optimisation of mass-produced structural steel products is widely researched. The objective is to minimise the quantity of material used without sacrificing the strength and practicality of the structural members. Current research focuses on optimising the dimensions of conventional cross-sectional shapes but rarely considers discovering new optimum shapes. This report introduces the concepts of a new optimisation method which enables the cross-section to self-shape to an optimum by using the evolution and adaptation benefits of Genetic Algorithm. The feasibility and accuracy of the method are verified by implementing it to find optimum thin-walled profiles against simple parameters for which analytical solutions are known, namely the optimisation of doubly-symmetric closed profiles. Results show that the cross-section accurately self-shapes to its optimum in a low number of generations. Factors influencing the convergence are presented and future challenges to applying the method to optimisation of cold-formed steel profiles with practical applications are discussed.

KEYWORDS

Optimisation, Genetic Algorithm, Thin-walled structures, Cold-formed steel structures

TABLE OF CONTENTS

1 INTRODUCTION

1.1 General

Cold-formed steel profiles are manufactured by bending a thin sheet of steel to a desired shape allowing efficient and light profiles to be used where conventional hot-rolled steel profiles prove uneconomic [1]. These members are mass-produced and commonly used in applications such as steel storage racks, roof and wall systems, composite concrete and steel slabs, or automotive parts.

One of the main advantages of cold-formed steel profiles is the great flexibility of cross-sectional shapes, attributable to the manufacturing process allowing achievement of almost any desired cross-section. The cross-sectional shape is the key element in enhancing the strength of cold-formed steel profiles as it controls the three fundamental buckling modes: local, distortional (for open profiles) and global. However, research on optimisation of cold-formed steel profiles has been restricted mainly to the conventional C, Z or Σ cross-sectional shapes [2-9] as shown Figure 1. Web and/or flange stiffeners (see Figure 1) used to avoid local instabilities were sometimes considered in the optimisation process. In these attempts the search areas were restricted, as new cross-sectional shapes were not considered, and only the dimension variables of the existing cross-sections were optimised (height, width and thickness). Therefore innovations are very limited.

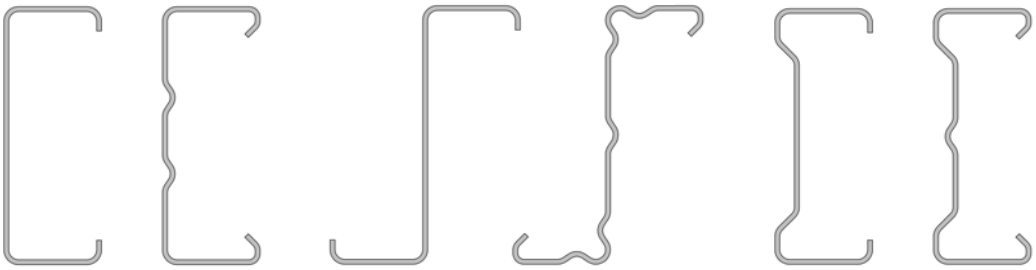

Figure 1: Cold-formed steel C, Z and Σ cross-sections with or without stiffeners

One can genuinely ask if cross-sectional shapes better than the conventional ones exist. Could one allow the cross-section to shape automatically in an optimal and natural way without being restricted to a narrow search area?

This report introduces the concepts of a new optimisation method that enables the cross-section to self-shape to an optimum by using the evolution and adaptation benefits of Genetic Algorithm. The feasibility and accuracy of the method are verified by implementing it to find optimum thin-walled profiles against simple parameters for which analytical solutions are known. This report constitutes the initial phase of a project aiming at finding practical and innovative cold-formed steel profiles without presumptions on the cross-sectional shapes, an optimisation process referred to as "shape discovery" [10]. Factors influencing the convergence are presented and future challenges to applying the method to optimisation of cold-formed steel profiles with practical applications are discussed herein.

1.2 Literature review, GA and "shape discovery"

Developed by John Holland [11] in the 1960s, Genetic Algorithm (GA) mimics the Darwin evolution theory of "survival of the fittest". GA enables searching optimum solutions efficiently, is suitable for highly non-linear problems, and does not require solving complex optimisation equations. GA is intended for unconstrained optimisation problems, although constraints (involved in most real world problems) are commonly introduced into the "fitness function" as penalty functions, see Section 2. GA has been successfully applied to a vast range of engineering and science disciplines [12-13], the literature featuring a wealth of articles demonstrating that GA can be an efficient and powerful optimisation method. In structural engineering, GA has been used to optimise frames and trusses [14-16] or steel and concrete structures [17-18], although only a limited number of parameters were optimised in these attempts.

Lu and Makelainen [19-21] and Lee et al. [6-7] used GA to optimise cold-formed steel hat, C and Σ profiles. However, in these works, GA was used as a traditional optimisation method, and only the dimensions of the profiles were optimised.

Research involving optimisation of un-predefined cross-sections have been carried out successfully by Griffiths and Miles [10] for hot-rolled steel profiles and Liu et. al. [22] for cold-formed steel profile. Griffiths and Miles [10] used GA and a voxel-based representation in which the design space was decomposed into a grid of identical sized squares. GA cross-over and mutation operators were not applied to the genotype strings but to the design space, allowing evolution and convergence to known optimum I and box profiles. Liu et al. [22] used a "knowledge-based global optimisation" which found promising cross-sections through the knowledge-based optimisation process, and further optimised using a gradient-based local optimisation process. The sections were limited to eight folds, and minor stiffeners adding strength to the profiles were not considered.

Recently, Leng et al [23] optimised the cross-sectional shapes of cold-formed steel open columns using three different optimisation algorithms, including traditional GA. Sections having a wall thickness of 1 mm and a perimeter of 280 mm were divided into 21 elements (i.e. an element width of 13.33 mm), and optimum "open circular" and "S" cross-sections were found. As in the case of Liu et al. [22], the length of the elements (about 14 times the profile thickness) may not allow small bending radii in the cross-sections and minor stiffeners to be created.

2 OPTIMISATION PROBLEM

Ragnedda and Serra [24] analytically investigated the optimum cross-section of a doubly symmetric thin-walled closed profile by minimising the cross-sectional area A_s for imposed second moments of area I_x and I_y about the two axes of symmetry. They showed that the optimum cross-section is an ellipse and therefore a circle of radius r if the two second moments of area I_x and I_y are equal. r is given as,

$$r = \sqrt[3]{I_x / \pi t} \tag{1}$$

where t is the wall thickness.

The feasibility and accuracy of the self-shape optimisation method proposed in this paper are verified herein by implementing it on the previous well known optimisation problem. As this particular problem is doubly-symmetric, only a quarter of the cross-section needs to be considered. The constrained optimisation problem, consisting of minimising the cross-sectional area A_s of the profile for given I_x and I_y, can be transformed into an unconstrained problem suitable for GA as,

$$\text{Minimise } f = \frac{A_s}{A_{optimum}} + \alpha_x \left| \frac{I_{sx}}{I_x} - 1 \right| + \alpha_y \left| \frac{I_{sy}}{I_y} - 1 \right| \tag{2}$$

where $A_{optimum}$ is the known optimum cross-sectional area, I_{sx} and I_{sy} are the second moments of area of the profile about the two axes of symmetry, α_x and α_y are the penalty factors. f is referred to as the fitness function and includes both the objective and the penalty functions.

3 SELF-SHAPE OPTIMISATION PRINCIPLE

The main characteristics of the self-shape optimisation principle are:

- The initial population in GA is generated by arbitrarily drawing cross-sections using self-avoiding random walks in a defined design space of dimension equal to x_{max} mm × y_{max} mm, as detailed in Section 3.2. The self-avoiding random walks enable the generation of cross-sections without presumptions of their shapes.
- Elitism is included in the optimisation process and the best two cross-sections of one generation are automatically copied to the next generation [21].

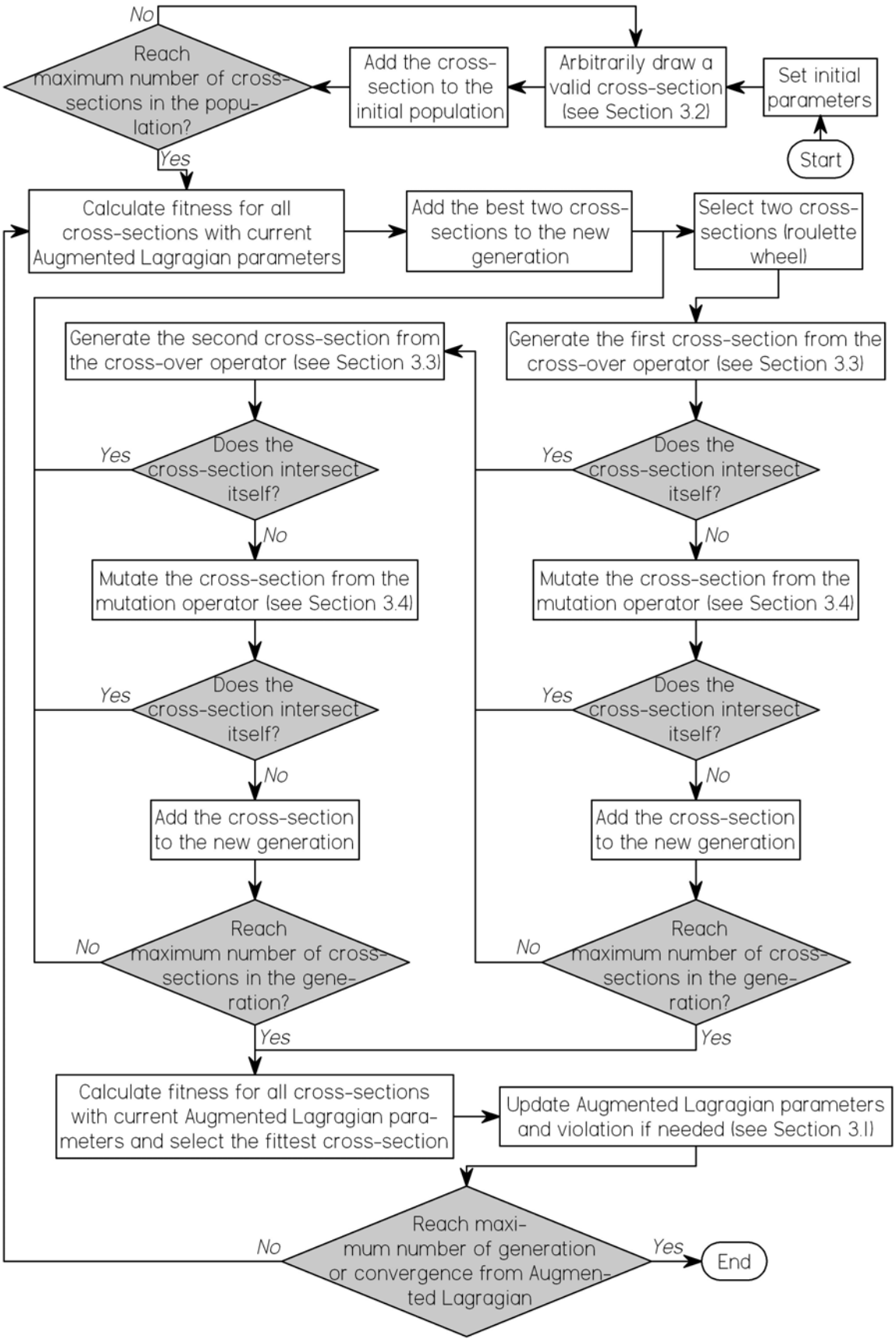

Figure 2: Global flowchart

- A floating-point type GA [25] is used in this research, meaning that a cross-section is not represented using typical binary strings but by floating-point numbers representing the coordinates of the points constituting the cross-section as,

$$\begin{bmatrix} X_i \\ Y_i \end{bmatrix} = \begin{bmatrix} 0, x_{i,2}, \ldots, x_{i,ni-1}, x_{i,ni} \\ y_{i,1}, y_{i,2}, \ldots, y_{i,ni-1}, 0 \end{bmatrix} \tag{3}$$

  where $[X_i, Y_i]$ is the coordinate vector of the i[th] cross-section with $x_{i,j}$ and $y_{i,j}$ being the x and y-coordinates, respectively, of the j[th] point of the cross-section. As only a quarter of the cross-section is analysed, the first point and the last point of the cross-section are forced to lie on the y and x-axes respectively.
- Cross-over and mutation operators are performed in relation to the design space and not to the floating-point variables, as detailed in Sections 3.3 and 3.4.
- Half of the population is allowed to enter the mating pool and the roulette wheel selection method is used.

A flowchart of the global algorithm is presented in Figure 2 with specific operations detailed in Sections 3.1 to 3.4

3.1 Augmented Lagragian method

Augmented Lagragian method for Genetic Algorithm has proven to be a powerful tool [19, 26] to avoid an ill-conditioned process by ensuring finite values of penalty factors. The method described in Adeli and Cheng [26] is used and the optimisation problem given in Section 2 is expressed as,

$$\text{Minimise } g = \frac{A_s}{A_{optimum}} + \frac{1}{2}\left(\gamma_x \left(\left| \frac{I_{sx}}{I_x} - 1 \right| + \mu_x \right)^2 + \gamma_y \left(\left| \frac{I_{sy}}{I_y} - 1 \right| + \mu_y \right)^2 \right) \tag{4}$$

where γ_x and γ_y are the penalty function coefficients and μ_x and μ_y are real parameters associated with each equality constraint. Initial values of $\gamma_x = \gamma_y = 2$ are used herein and found to be adequate as shown in Section 4.1.4. Initial values of $\mu_x = \mu_y = 0$ are used as recommended in [27].

A penalty increasing constant $\beta = 1.05$ is used to avoid premature convergence of the algorithm due to high values of β were used, as investigated in Section 4.1.3. The convergence rate α is set to 1.5 [26].

The augmented Lagragian method consists of the following steps [26]:

Step 1: Initialise the penalty function coefficients, $\gamma_x = \gamma_y = 2$, the real parameters associated with each equality constraint, $\mu_x = \mu_y = 0$ and the violation constraint $Viol_{previous} = \infty$. Set the penalty increasing constant $\beta = 1.05$, the convergence rate $\alpha = 1.5$ and the stopping criteria $\varepsilon = 10^{-6}$.

Step 2: Run the Genetic Algorithm (see Figure 2) and obtain the second moments of area $I_{sx,best}$ and $I_{sy,best}$ of the fittest cross-section determined from Eq. (4).

Step 3: Calculate the current violation constraint $Viol_{current} = max\left(\left| \frac{I_{sx,best}}{I_x} - 1 \right|, \left| \frac{I_{sy,best}}{I_y} - 1 \right| \right)$

Step 4: Check convergence of the algorithm as,
- a) If $Viol_{current} < \varepsilon$, stop the algorithm, the fittest solution found in Step 2 is the solution
- b) Else if $Viol_{current} > Viol_{previous}$, go to Step 5.
- c) Else if $Viol_{current} \leq Viol_{previous}$, go to Step 6.

Step 5: Update the penalty function coefficients and real parameters associated with each equality constraint as,

a) If $\left| \frac{I_{sx,best}}{I_x} - 1 \right| \geq \frac{Viol_{previous}}{\alpha}$ do $\gamma_x = \beta\gamma_y$ and $\mu_x = \frac{\mu_x}{\beta}$

b) If $\left| \frac{I_{sy,best}}{I_y} - 1 \right| \geq \frac{Viol_{previous}}{\alpha}$ do $\gamma_y = \beta\gamma_y$ and $\mu_y = \frac{\mu_y}{\beta}$

c) Go to Step 2.

Step 6: Update the penalty function coefficients and real parameters associated with each equality constraint as,

a) $\mu_x = \mu_x + \left|\frac{I_{sx,best}}{I_x} - 1\right|$ and $\mu_y = \mu_y + \left|\frac{I_{sy,best}}{I_y} - 1\right|$

b) If $Viol_{current} \geq Viol_{previous}/\alpha$ then,

b1) If $\left|\frac{I_{sx,best}}{I_x} - 1\right| \geq \frac{Viol_{previous}}{\alpha}$ do $\gamma_x = \beta\gamma_x$ and $\mu_x = \frac{\mu_x}{\beta}$

b2) If $\left|\frac{I_{sy,best}}{I_y} - 1\right| \geq \frac{Viol_{previous}}{\alpha}$ do $\gamma_y = \beta\gamma_y$ and $\mu_y = \frac{\mu_y}{\beta}$

c) $Viol_{previous} = Viol_{current}$ and go to Step 2.

Steps 3 to 5 are referred to as the inner loop and Step 6 is referred to as the outer loop.

3.2 Initial population

Cross-sections are drawn using self-avoiding random walks on a x_{max} mm × y_{max} mm design space, based on the following rules allowing arbitrary and continuous cross-sections to be drawn:

Step 1: a) A random point is chosen on the vertical axis (y-axis) in the interval [0, y_{max}] (see Figure 3 (a)).

b) An element of nominal size of 1 mm is created from the previous built point in the direction randomly chosen between -45° to 45° to the horizontal (see Figure 3 (a)).

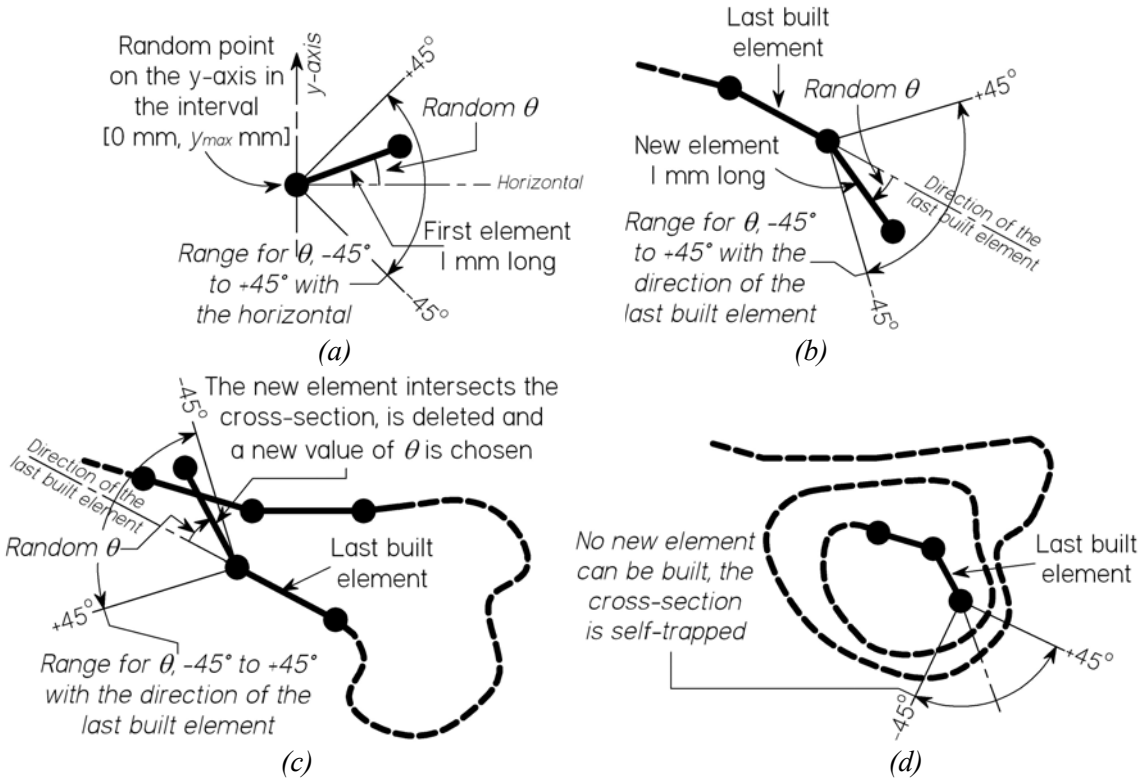

Figure 3: Creating the initial cross-sections, (a) Step 1, (b) Step 2, (c) Step 3 a) and self-trapped cross-section

Step 2: A new element of nominal size of 1 mm is created from the last built element in the direction randomly chosen between -45° to 45° to the orientation of the last built element (see Figure 3 (b)).

Step 3: Perform the following checks:

a) If the last built element intersects the cross-section (i.e. the cross-section is not self-avoiding) or the axes x = 0, x = x_{max} or y = y_{max} (i.e. the boundaries of the design space), then delete that element and go to Step 2 (see Figure 3 (c)).

b) Else if the element intersects the axis y = 0, then stop building the cross-section. The cross-section is considered to be valid and is added to the initial population.

c) Otherwise go to Step 2.

The nominal size of the elements is set to 1 mm, which corresponds to the wall thickness of all profiles used to validate the method in Section 4. The size of the elements and its relationship with the internal bending radius is discussed in section 5.2 for future cold-formed steel applications.

Self-avoiding random walks can self-trap (see Figure 3 (d)) and a cross-section is considered self-trapped if Step 3 a) is repeated 10 times in a row. The cross-section is then considered unfit and not added to the initial population. Initial cross-section examples are shown in Figure 4 on a 40 mm × 40 mm design space.

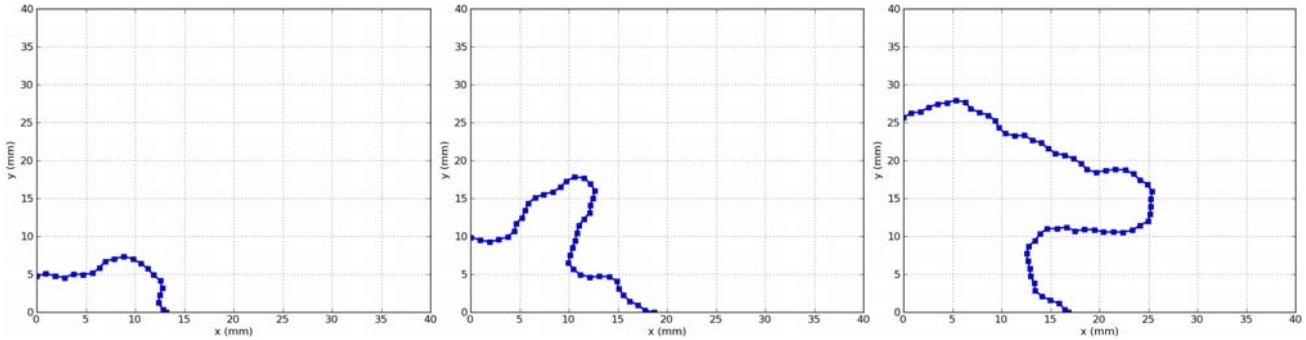

(a) *(b)* *(c)*

Figure 4: Initial cross-section on a 40 mm × 40 mm design space of (a) 20 elements, (b) 40 elements and (c) 60 elements

3.3 Cross-over operator

A one-point cross-over operator type is used herein. Two points $P_{parent1}$ and $P_{parent2}$ are chosen at δ % along the length of the first and second parents, respectively, with δ being a random number in the interval]0,100[. Two points P_1 and P_2, as shown in Figure 5 (a), are then defined using a linear interpolation between $P_{parent1}$ and $P_{parent2}$ as,

$$P_1 = \lambda P_{Parent1} + (1-\lambda) P_{parent2} \quad \text{and} \quad P_2 = \lambda P_{Parent2} + (1-\lambda) P_{parent1} \tag{5}$$

where λ is a random number in the interval [0,1]. Eq. (5) allows new materials to be added in subsequent generations [25].

Two offsprings are created per operation with the first offspring built using the right-hand part of the first parent and the left-hand part of the second parent as,

Step 1: The right-hand part of the first parent is rotated about its intersection point P_{y1} with the y-axis and scaled so that the last point $P_{parent1}$ of the part matches point P_1 as illustrated in Figure 5 (b).

Step 2: The left-hand part of the second parent is rotated about its intersection point P_{x2} with the x-axis and scaled so that the first point $P_{parent2}$ of the part matches point P_1 as illustrated in Figure 5 (b).

Step 3: The two parts created in Steps 1 and 2 are added together in Figure 5 (b).

Step 4: Elements constituting the offspring are merged or subdivided to keep all elements about 1 mm long, in the interval [0.75 mm, 1.5 mm].

Step 5: If the created cross-section intersects itself, the offspring is considered unfit and is disregarded as illustrated in Figure 2.

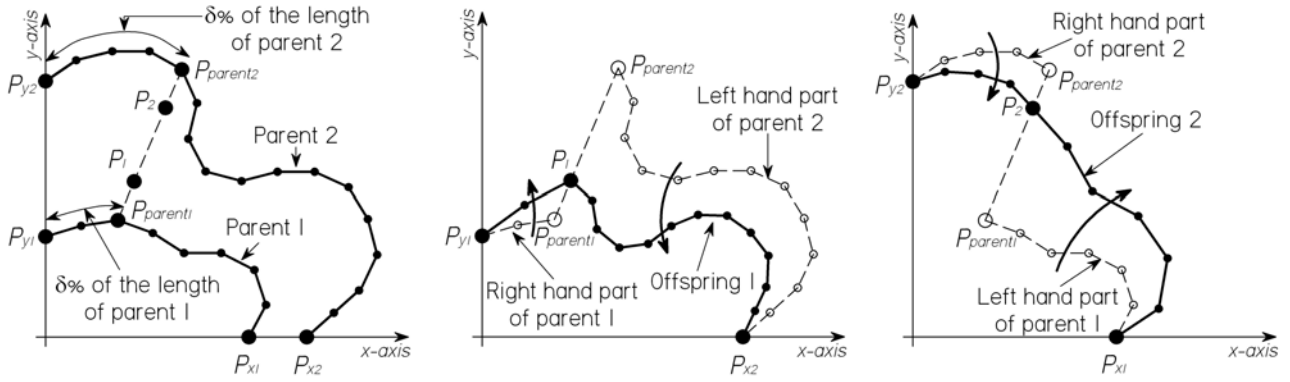

Figure 5: Cross-over operator (a) defining cross-over points, (b) first offspring and (c) second offspring

The second offspring is similarly based on the left hand part of the first parent and the right hand part of the second parent using point P_2 instead of P_1 (see Figure 5 (c)). Offsprings are created until the overall population is replaced (see in Figure 2). A typical cross-over probability of 0.8 is used.

3.4 Mutation operator

Mutation allows new cross-sectional shapes to be introduced into the population by redrawing a part or several parts of a cross-section. The operator acts on the points constituting the cross-sections with a typical mutation probability of 0.01 for each point. If a point mutates, the part of the cross-section around that point is redrawn as,

Step 1: A number of elements is randomly chosen in the interval [1, 0.25 × the number of elements constituting the cross-section] and deleted on each side of the mutated point (see Figure 6).

Step 2: A new arbitrary, self-avoiding and continuous shape is drawn in an infinite design space based on the principles detailed in Section 3.2 with the exception of Step 3 b) (see Figure 6). The number of elements constituting this shape is twice the number of elements chosen in Step 1.

Step 3: a) If the number of elements between the intersections of the initial cross-section with the x-axis (point P_x) or the y-axis (point P_y) is greater than the number of element chosen in Step 1, go to Step 4.
b) Else go to Step 5.

Step 4: The created shape in Step 2 is inserted in the cross-section in lieu of the elements deleted in Step 1 (see Figure 6 (a)). Go to Step 6.

Step 5: a) A new point is defined on the x- or y-axis at a distance ±d from point P_x or P_y respectively, where d is randomly chosen in the interval [0, nominal size of one element × (number of elements chosen in Step 1 - number of elements between the mutated point and point P_x or P_y)]
b) The created shape in Step 2 is inserted in the cross-section between the new point defined in Step 5 a) and the first point of the cross-section not deleted in Step 1 (see Figure 6 (b)).

Step 6: Elements constituting the mutated part are merged or subdivided to keep all elements about 1 mm long, in the interval [0.75 mm, 1.5 mm].

A number of elements deleted and redrawn equal to a maximum of 50% of the number of elements constituting the cross-section was found to provide good results as investigated in Section 4.1.2. If the mutated cross-section intersects itself, the cross-section is considered unfit and is disregarded as shown in Figure 2. A new cross-section is then created from the cross-over and mutation operators to maintain the size of the population.

Step 5 allows cross-sections to intersect the x- or y-axes at new locations and overcomes this deficiency in the cross-over operator. The further the mutated point is from the intersection points P_x or P_y of the cross-section with the x- or y-axis, the closer the new point is to point P_x or P_y.

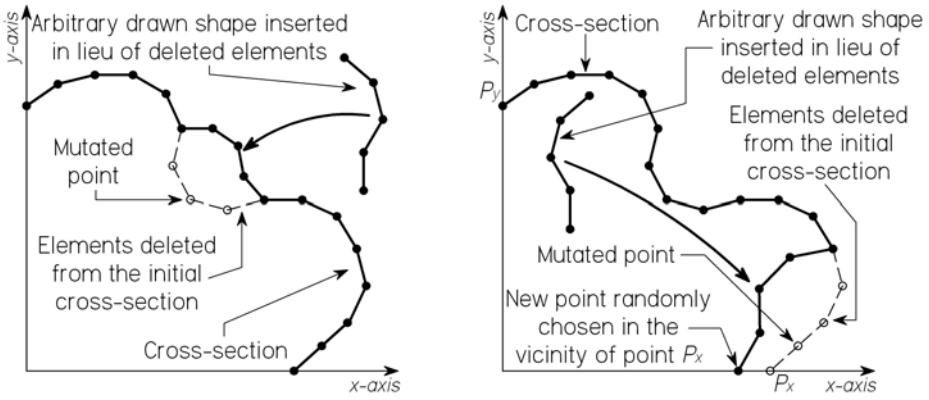

Figure 6: Mutation operator (a) in the middle part of the cross-section and (b) next to the intersection point P_x with the x-axis

4 RESULTS

4.1 20 mm radius circle

A 20-mm radius circle with 1 mm wall thickness is used in this section to validate the self-shape optimisation principle. The design space is set to be 40 mm × 40 mm, i.e. twice the radius of the circle.

The cross-sectional areas of the initial population are deliberately generated to be evenly distributed between 10 elements (cross-sectional area = 40 mm^2 – about one third of the optimum cross-sectional area) and 60 elements (cross-sectional area = 240 mm^2 – about twice the optimum cross-sectional area) allowing diversity within the initial population, as investigated in Section 4.4. The cross-sections are uniformly distributed in five categories of 10 elements each.

The influence of the population size, the maximum number of elements redrawn in the mutation operator nd the penalty increasing constant β and initial penalty function coefficients γ_x and γ_y in the Augmented Lagragian method on the convergence of the algorithm is investigated in this Section.

4.1.1 Influence of the population size

Figure 7 plots the average fitness function f given in Eq. (2) for 10 runs with penalty factors α_x = α_y = 10 for population sizes of 400, 700 and 1000 cross-sections. Values of $A_{optimum}$, I_x and I_y in Eq. (2) are given in Table 1 as main parameters used in the GA. Detailed results are summarised in Appendix 1.

The average errors, over 10 runs, in cross-sectional area and second moments of area are given in Table 2. For all population sizes, the algorithm accurately finds the optimum circle with average errors over 10 runs at the 100th generation ranging between 0.25% and 0.50% for the cross-sectional area and between 0.01% and 0.04% for the targeted second moments of area, with the population size of 1000 cross-sections giving slightly better results. As seen in Figure 7, about 50 generations are needed for the algorithm to converge to a near optimum solution.

The size of the population has little influence on the accuracy and convergence of the algorithm and a population size of 700 cross-sections is chosen for further analysis.

Table 1: Main parameters used in investigating the influence of the population size

Optimum section properties			Augmented Lagragian parameters in Section 3.1				Other parameters	
Radius (mm)[(1)]	$A_{optimum}$ (mm^2)	I_x, I_y (mm^4)	Initial γ_x, γ_y	Initial μ_x, μ_y	β	α	Design space (mm × mm)	Mutation length (%)[(2)]
20	125.7	25,148.4	2	0	1.05	1.5	40 × 40	50

[(1)]: the radius is measured at the neutral axis of the wall thickness
[(2)]: maximum number of elements redrawn in the mutation operator relative to the number of elements of the cross-section

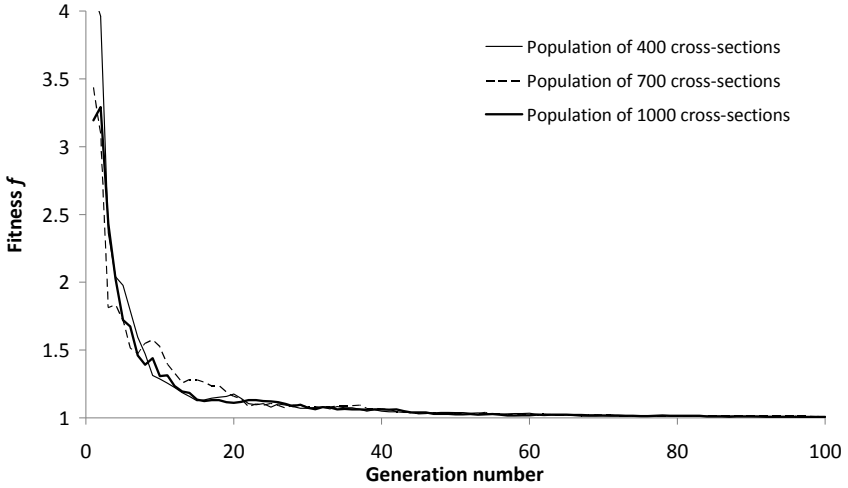

Figure 7: Average fitness f for various population sizes

Table 2: Average results at the 100th generation for various population sizes

	Results over 10 runs at the 100th generation					
Population (number of cross-sections)	A_s Aver. error (%)	CoV	I_{sx} Aver. error (%)	CoV	I_{sy} Aver. error (%)	CoV
400	0.50	0.0023	0.02	0.0002	0.01	0.0001
700	0.30	0.0015	0.02	0.0002	0.04	0.0005
1000	0.25	0.0005	0.02	0.0002	0.02	0.0001

Figure 8 shows the evolution of the cross-section for one solution and a population size of 700 cross-sections. For clarity the entire design space of 40 mm × 40 mm is not represented in Figure 8.

4.1.2 Influence of the maximum mutation length

Figure 9 plots the average fitness function *f* given in Eq. (2) for 10 runs with penalty factors α_x = α_y = 10 for a maximum number of elements deleted and redrawn in the mutation operator equal to 30%, 50% and 70% of the number of elements constituting the cross-section. The main parameters used in the optimisation process are summarised in Table 3. Detailed results are summarised in Appendix 2.

The average errors, over 10 runs, in cross-sectional area and second moments of area are given in Table 4. The algorithm accurately finds the optimum circle with an average error over 10 runs at the 100th generation of about 0.30% for the cross-sectional area and 0.03% for the targeted second moments of area, for all maximum mutation lengths.

The size of the maximum mutation length has little influence on the accuracy and convergence of the algorithm and is chosen to 50% of the length of the cross-section for further analysis.

Table 3: Main parameters used in investigating the influence of the maximum mutation length

Optimum section properties			Augmented Lagragian parameters in Section 3.1				Other parameters	
Radius (mm)[(1)]	$A_{optimum}$ (mm^2)	I_x, I_y (mm^4)	Initial γ_x, γ_y	Initial μ_x, μ_y	β	α	Design space (mm × mm)	Population (nb of cross-section)
20	125.7	25,148.4	2	0	1.05	1.5	40 × 40	700

[(1)]: the radius is measured at the neutral axis of the wall thickness

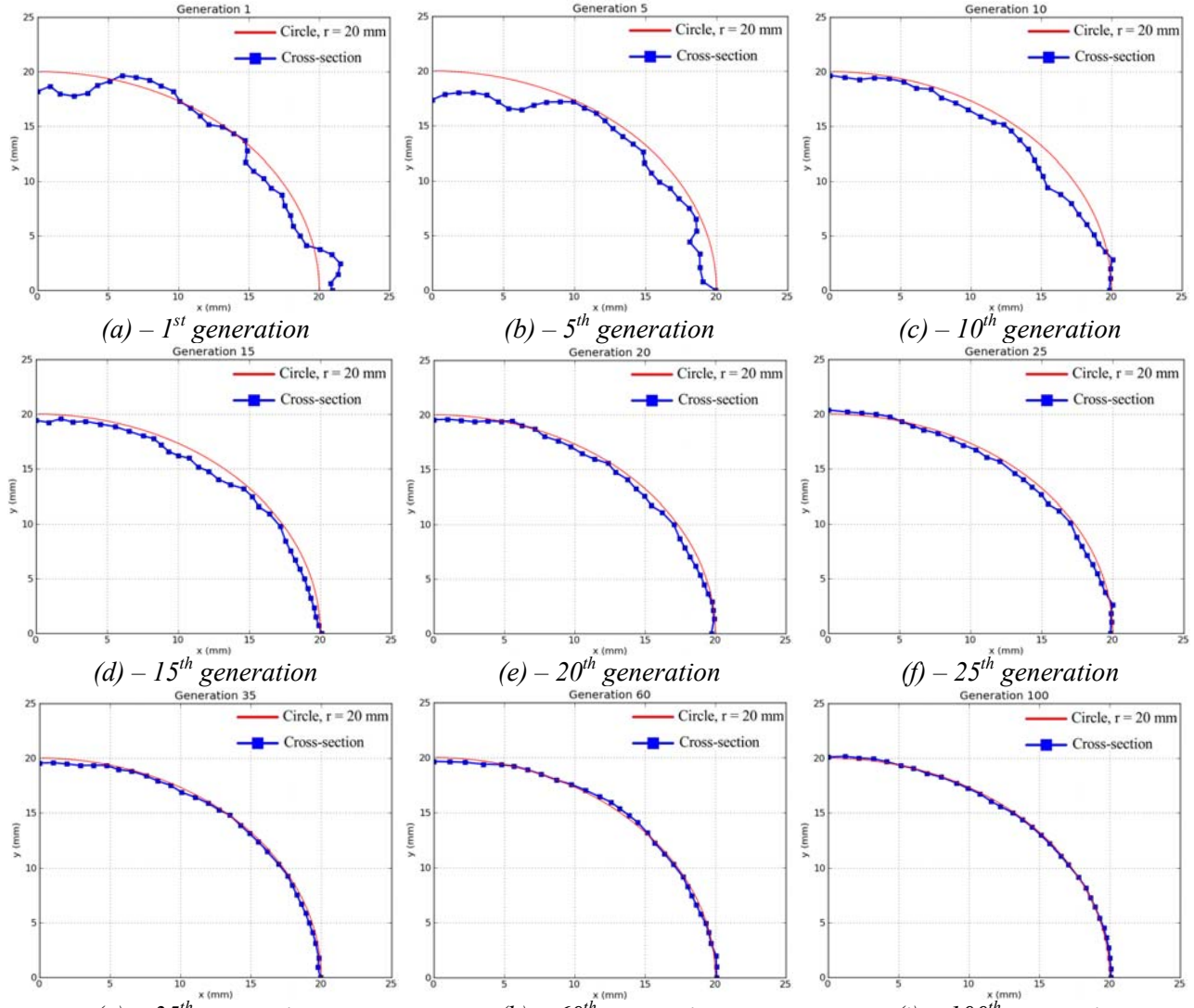

(a) – 1st generation *(b) – 5th generation* *(c) – 10th generation*

(d) – 15th generation *(e) – 20th generation* *(f) – 25th generation*

(g) – 35th generation *(h) – 60th generation* *(i) – 100th generation*

Figure 8: Fittest cross-sections for a population size of 700 cross-sections from (a) 1st generation (initial population) to (i) 100th generation

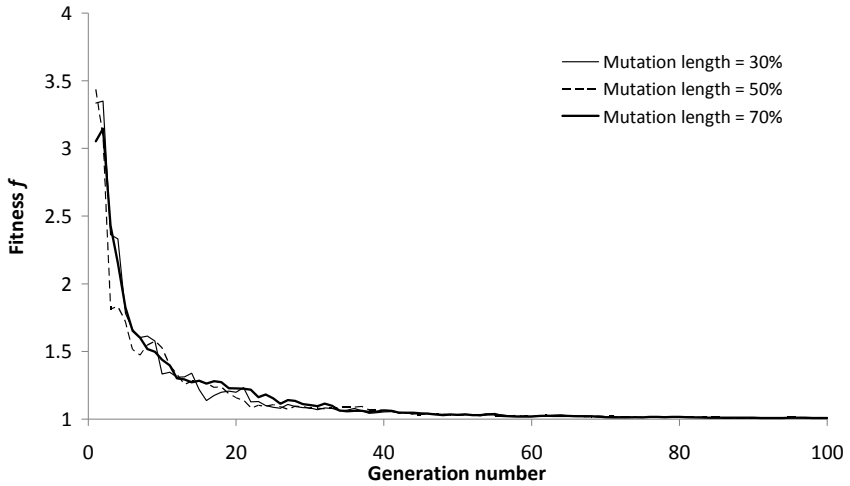

Figure 9: Average fitness f for various maximum mutation lengths

Table 4: Average results at the 100th generation for various maximum mutation lengths

	Results over 10 runs at the 100th generation					
	A_s		I_{sx}		I_{sy}	
Mutation length (%)	Aver. error (%)	CoV	Aver. error (%)	CoV	Aver. error (%)	CoV
30	0.30	0.0017	0.03	0.0004	0.02	0.0002
50	0.30	0.0015	0.02	0.0002	0.04	0.0005
70	0.29	0.0013	0.04	0.0002	0.03	0.0001

4.1.3 Influence of the penalty increasing constant β

The penalty increasing constant β increases the weight of the equality constraints in Eq. (4) if the constraints are greater than a violation criterion, as shown in Section 3.1. The greater the constant β, the greater the increase in the weight of the equality constraints in the fitness function g in Eq. (4) [26]. This section investigates the accuracy of the algorithm for various value of β.

Figure 10 plots the average fitness function f given in Eq. (2) for 10 runs with penalty factors $\alpha_x = \alpha_y = 10$ and for penalty increasing constant β ranging from 1.01 to 10 in the Augmented Lagragian method. The main parameters used in the optimisation process are summarised in Table 5. Detailed results are given in Appendix 3.

The average errors, over 10 runs, in cross-sectional area and second moments of area are given in Table 6. For value of β greater than 1.1, the algorithm tends to satisfy the equality constraints too rapidly and converges to local optimums with an average error over 10 runs on the cross-sectional area of up to 8.94% for $\beta = 10$. Typical solutions for $\beta = 10$ at the 100th generation are given in Figure 11.

Table 5: Main parameters used in investigating the influence of the maximum mutation length

Optimum section properties			Augmented Lagragian parameters in Section 3.1			Other parameters		
Radius (mm)[(1)]	$A_{optimum}$ (mm^2)	I_x, I_y (mm^4)	Initial γ_x, γ_y	Initial μ_x, μ_y	α	Design space (mm × mm)	Mutation length (%)[(2)]	Population (nb of cross-section)
20	125.7	25,148.4	2	0	1.5	40 × 40	50	700

[(1)]: the radius is measured at the neutral axis of the wall thickness
[(2)]: maximum number of elements redrawn in the mutation operator relative to the number of elements of the cross-section

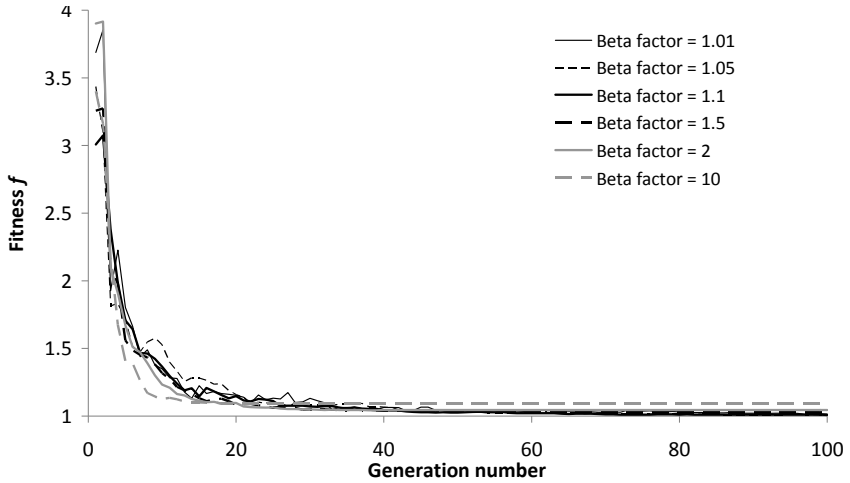

Figure 10: Average fitness f for various β factors

The value of the penalty increasing constant β is found to significantly influence the accuracy of the algorithm. A value of β equal to 1.05 allows the algorithm to explore the design space before converging and is chosen for further analysis. This value of β is significantly less than the value of 10 recommended by Belegundu and Arora [27] and Bazaraa et. al. [28].

Table 6: Average results at the 100th generation for various β factors

	Results over 10 runs at the 100th generation					
	A_s		I_{sx}		I_{sy}	
β factor	Aver. error (%)	CoV	Aver. error (%)	CoV	Aver. error (%)	CoV
1.01	0.31	0.0018	0.06	0.0010	0.07	0.0012
1.05	0.30	0.0015	0.02	0.0002	0.04	0.0005
1.1	0.51	0.0038	0.03	0.0002	0.01	0.0002
1.5	2.98	0.0062	0.00	0.0000	0.00	0.0000
2	4.43	0.0147	0.00	0.0000	0.00	0.0000
10	8.94	0.0230	0.00	0.0000	0.00	0.0000

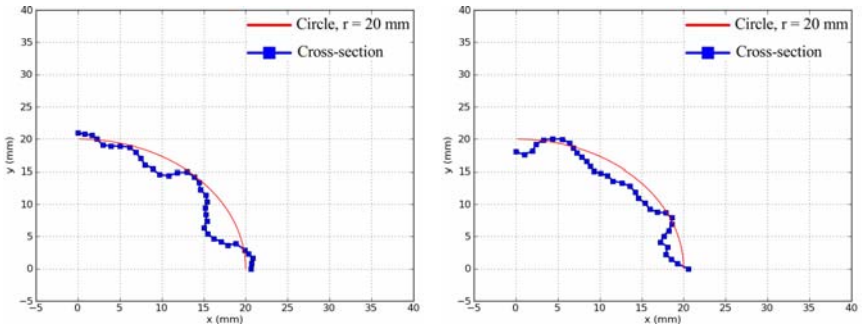

(a) *(b)*

Figure 11: Typical solutions for penalty increasing constant β = 10 at the 100th generation

4.1.4 Influence of the penalty function coefficients γ_x and γ_y

Figure 12 plots the average fitness function *f* given in Eq. (2) for 10 runs with penalty factors α_x = α_y = 10 and for penalty function coefficients γ_x and γ_y in the Augmented Lagragian method ranging from 0.35 to 5. The main parameters used in the optimisation process are given in Table 7. Detailed results are summarised in Appendix 4.

The average errors, over 10 runs, in cross-sectional area and second moments of area are given in Table 8. For all values of γ_x and γ_y, the algorithm accurately finds the optimum circle with an average error over 10 runs at the 100th generation of about 0.30% for the cross-sectional area and 0.03% for the targeted second moments of area. However, for small values of the penalty function coefficients (0.35 and 0.5), the algorithm selects cross-sections having a relatively small number of

elements as the fittest cross-sections in the first generations, because the initial weight of the penalty functions is much less that the weight of the objective function in Eq. (4). This selection continues until the real parameters associated with each equality constraint are updated in the outer loop of the Augmented Lagragian method presented Section 3.1. Figure 13 shows typical fittest cross-sections within the first generations for γ_x = γ_y = 0.35. For values of γ_x and γ_y less than 0.35, the algorithm does not converge and keep selecting cross-sections having a small number of elements as fittest cross-sections for all generations.

Table 7: Main parameters used in investigating the influence of the penalty function coefficients

Optimum section properties			Augmented Lagragian parameters in Section 3.1			Other parameters		
Radius (mm)[(1)]	$A_{optimum}$ (mm^2)	I_x, I_y (mm^4)	Initial μ_x, μ_y	α	β	Design space (mm × mm)	Mutation length (%)[(2)]	Population (nb of cross-section)
20	125.7	25,148.4	0	1.5	1.05	40 × 40	50	700

[(1)]: the radius is measured at the neutral axis of the wall thickness
[(2)]: maximum number of elements redrawn in the mutation operator relative to the number of elements of the cross-section

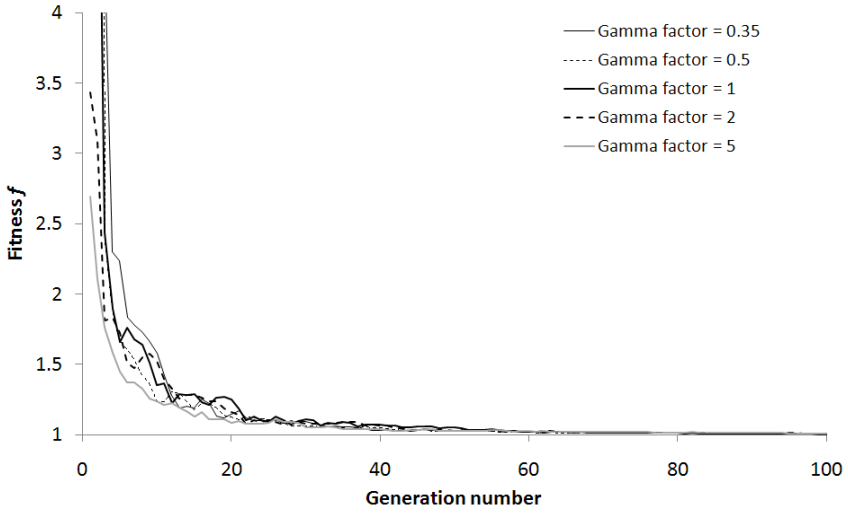

Figure 12: Average fitness f for various penalty function coefficients

The value of the penalty function coefficients is found to influence the behaviour of the algorithm in the first generations and a value of γ_x = γ_y = 2 is chosen for further analysis.

Table 8: Average results at the 100th generation for various penalty function coefficients

	Results over 10 runs at the 100th generation					
Penalty function coeff. γ_x and γ_y	A_s Aver. error (%)	A_s CoV	I_{sx} Aver. error (%)	I_{sx} CoV	I_{sy} Aver. error (%)	I_{sy} CoV
0.35	0.27	0.0010	0.01	0.0001	0.02	0.0002
0.5	0.31	0.0017	0.02	0.0002	0.02	0.0001
1	0.23	0.0013	0.01	0.0001	0.01	0.0002
2	0.30	0.0015	0.02	0.0002	0.04	0.0005
5	0.50	0.0015	0.03	0.0002	0.02	0.0002

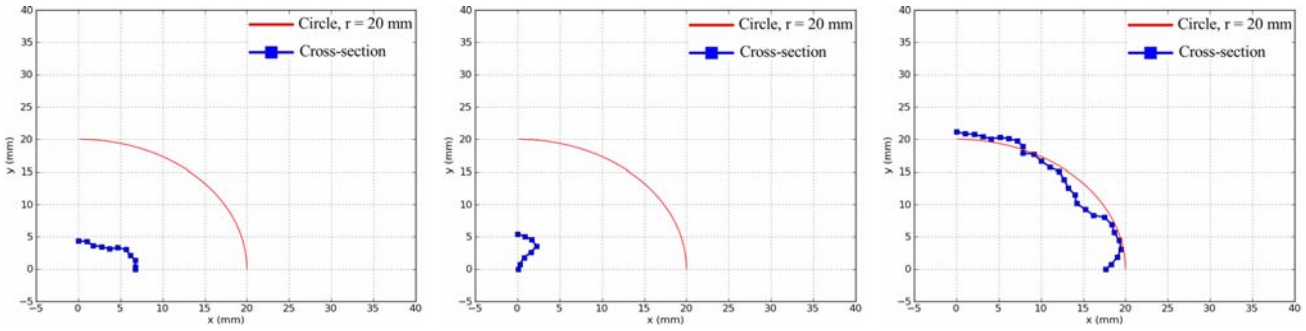

(a) *(b)* *(c)*

Figure 13: Typical fittest cross-sections for $\gamma_x = \gamma_y = 0.35$ (a) 1st generation (initial population), (b) 2nd generation and (c) 3rd generation

4.2 Various radius circles

The self-shape optimisation principle is checked in this section against optimum cross-sections corresponding to circles of radius ranging from 10 mm to 40 mm. All cross-sections have a wall thickness of 1 mm.

For each optimisation problem, the design space is set to be $2r \times 2r$, where r is the radius of the optimum circle, as shown in Table 9. Cross-section areas in the initial population are uniformly distributed between 0 mm^2 (r = 10 mm) or 40 mm^2 (r = 20 mm, 30 mm and 40 mm) and about twice the cross-sectional area of the optimum circle as shown in Table 9.

Table 9: Main parameters used in investigating the accuracy of the algorithm on various radius circles

Optimum section properties			Initial population distribution			Other parameters	
Radius (mm)[(1)]	$A_{optimum}$ (mm^2)	I_x, I_y (mm^4)	Min. cross-sectional area (mm^2)	Max. cross-sectional area (mm^2)	Number of categories	Design space (mm × mm)	Population (nb of cross-section)
10	62.8	3,149.5	0	200	5	20 × 20	700
20	125.7	25,148.4	40	240	5	40 × 40	700
30	188.5	84,846.6	40	400	9	60 × 60	702
40	251.3	201,093.4	40	480	11	80 × 80	704

(1): the radius is measured at the neutral axis of the wall thickness

Figure 14 plots the average fitness function f given in Eq. (2) for 10 runs with penalty factors $\alpha_x = \alpha_y = 10$ for the optimisation problems given above. Detailed results are given in Appendix 5.

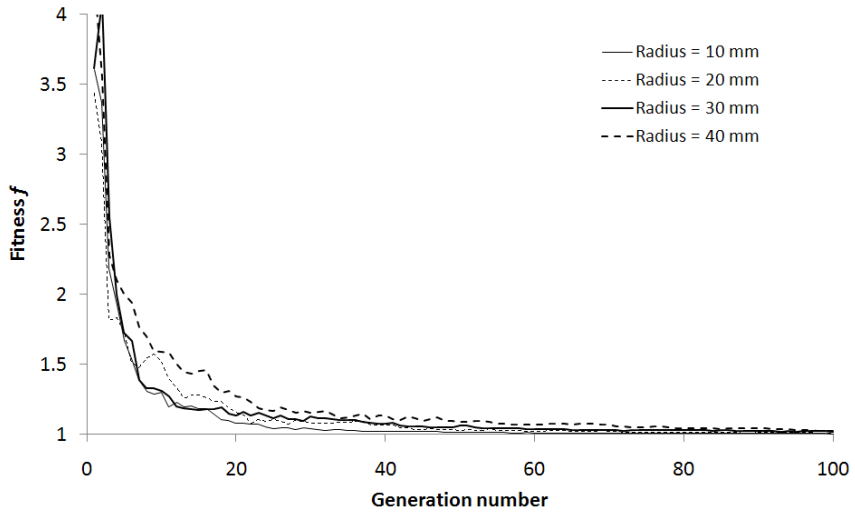

Figure 14: Average fitness f for various radius circles

The average errors, over 10 runs, in cross-sectional area and second moments of area are given in Table 10. As the radius of the targeted optimum solution increases, the proposed GA keeps satisfying the constraints but moves away from the optimum cross-section. For the 40 mm radius circle, the average error for the cross-sectional area, over 10 runs, at the 100th generation is still reasonable and equal to 1.63% with a coefficient of variation of 0.0032. Figure 15 shows typical solutions for the 40 mm radius circle. For clarity, the entire design space in not shown in Figure 15.

The increase in the average error in the cross-sectional area with increasing radius r of the targeted optimum solution is mainly related to the size of the design space and the number of elements constituting the cross-section. The size of the design space varies quadratically while the cross-sectional area varies almost linearly with the radius r. Therefore, as the value of r increases, the algorithm has to investigate an increased number of solutions for a given accuracy.

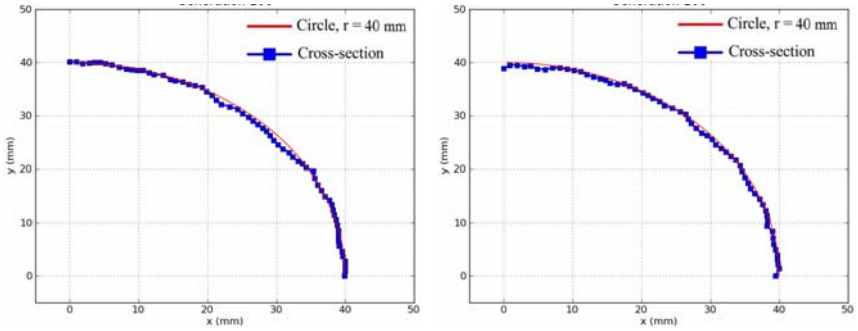

(a) *(b)*

Figure 15: Typical fittest cross-sections for optimum circle of 40 mm radius at the 100th generation

The computational time is increased by a factor 11.3 between the 20 mm (32 elements) and the 40 mm (63 elements) radius circles with an average CPU time of 0.65 hour against 7.32 hours per run on a 3 GHz Intel Core2 Quad processor. The computation time is discussed in Section 5 for future applications.

Table 10: Average results at the 100th generation for various radius circles

	Results over 10 runs at the 100th generation					
Optimum radius	A_s		I_{sx}		I_{sy}	
(mm)	Aver. error (%)	CoV	Aver. error (%)	CoV	Aver. error (%)	CoV
10	0.24	0.0013	0.01	0.0001	0.01	0.0001
20	0.30	0.0015	0.02	0.0002	0.04	0.0005
30	0.87	0.0030	0.04	0.0006	0.04	0.0004
40	1.63	0.0032	0.03	0.0002	0.07	0.0008

4.3 Ellipses

The self-shape optimisation principle is verified in the section against minimising the cross-sectional area with different targets of the second moments of area about the two axes of bending. As mentioned in Section 2, the optimum cross-section is an ellipse of radii r_x and r_y along the x- and y-axes, respectively.

An ellipse of radii r_x = 30 mm and r_y = 15 mm with a wall thickness of 1 mm is used as the solution to the optimisation problem, with cross-sectional properties given in Table 11. The design space is set to be 60 mm × 30 mm and corresponds to twice the radii r_x and r_y of the ellipse. The initial population is uniformly distributed between cross-sectional areas of 40 mm^2 (about one-third of the optimum cross-sectional area) and 240 mm^2 (about twice the optimum cross-sectional area).

Table 11: Main parameters used in investigating the influence of the maximum mutation length

Optimum section properties					Other parameters	
r_x (mm)[(1)]	r_y (mm)[(1)]	$A_{optimum}$ (mm^2)	I_x (mm^4)	I_y (mm^4)	Design space (mm × mm)	Population (nb of cross-section)
30	15	141.4	18569.8	53035.0	60 × 30	700

(1): the radius is measured at the neutral axis of the wall thickness

Figure 16 plots the average fitness function *f* given in Eq. (2) for 10 runs with penalty factors α_x = α_y = 10 for the optimisation problem given above. The main parameters used in the optimisation process are summarised in Table 11. Detailed results are given in Appendix 6.

The average errors, over 10 runs, in cross-sectional area and second moments of area are given in Table 12. The algorithm finds the optimum ellipse with an average error over 10 runs at the 100th generation of 2.08% for the cross-sectional area and 0.05% for the second moments of area. Figure 17 shows typical solutions at the 100th generation. For clarity, the entire design space in not shown in Figure 17.

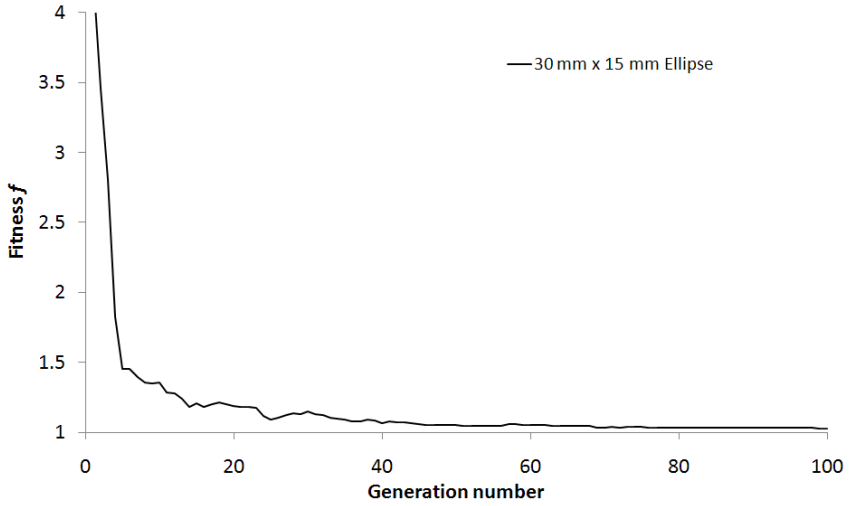

Figure 16: Average fitness f for a 30 mm × 15 mm ellipse

Table 12: Average results at the 100th generation for a 30 mm × 15 mm ellipse

	Results over 10 runs at the 100th generation					
Ellipse r_x × r_y	A_s		I_{sx}		I_{sy}	
(mm × mm)	Aver. error (%)	CoV	Aver. error (%)	CoV	Aver. error (%)	CoV
30 × 15	2.08	0.0017	0.04	0.0002	0.07	0.0006

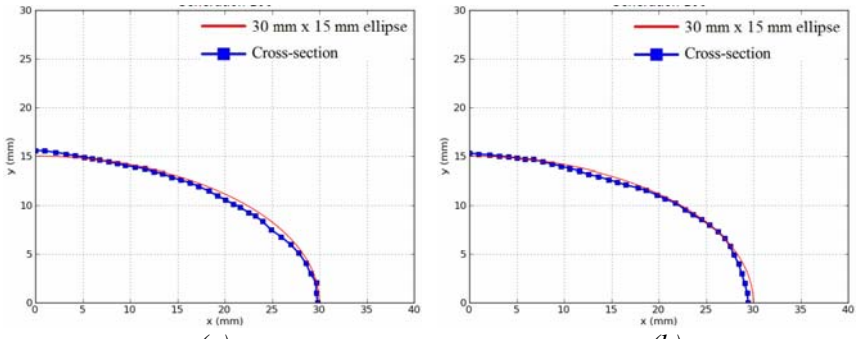

(a) *(b)*

Figure 17: Typical fittest cross-sections for a 30 mm × 15 mm ellipse at the 100th generation

4.4 Distribution of the initial population

Figure 18 plots the distribution (non uniform distribution) of the cross-sectional areas in the initial population when cross-sections are generated by only rejecting self-trapped cross-sections as mentioned in Section 3.2. The longer the cross-section, the higher the probability the cross–section has to self-trap when being created. Consequently, short cross-sections are over represented in the initial population and diversity within the initial population is not permitted, see Figure 18.

This section investigates the influence of forcing or not the cross-sectional areas to be uniformly distributed within the initial population. For uniformly distributed initial population, cross-sections are created as described in Section 3.2, disregarded or added to the initial population to match the desired distribution. The optimisation problem investigated in Section 4.2 for optimum solutions of radii equal to 20 mm and 30 mm is used herein. Initial cross-sections are either non uniformly distributed as shown in Figure 18 or uniformly distributed as given in Table 9 and shown in Figure 18.

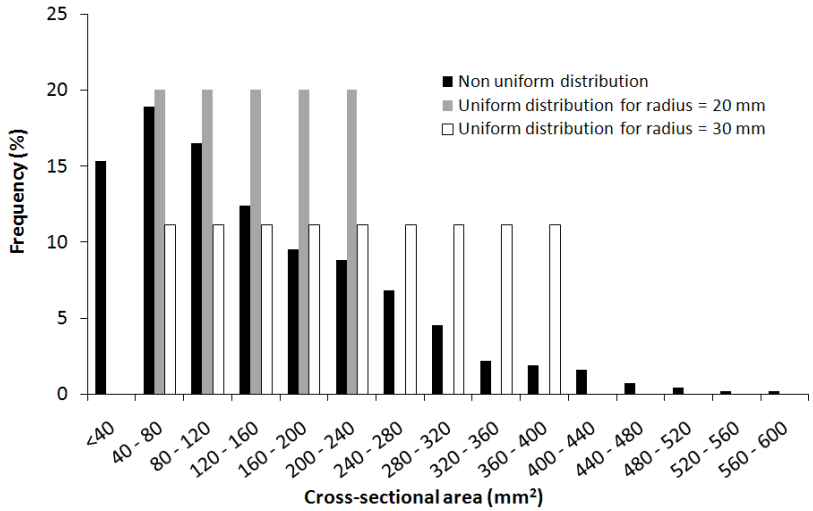

Figure 18: Cross-section areas distribution

Figure 19 plots the average fitness function f given in Eq. (2) for 10 runs with penalty factors α_x = α_y = 10 for the optimisation problem given above. The main parameters used in the optimisation process are summarised in Table 13. Detailed results are given in Appendix 7.

Table 13: Main parameters used in investigating the influence of the distribution of the initial population

Optimum section properties			Initial population distribution				Other parameters	
Radius (mm)[(1)]	$A_{optimum}$ (mm^2)	I_x, I_y (mm^4)	Distribution type	Min. cross-sectional area (mm^2)	Max. cross-sectional area (mm^2)	Number of categories	Design space (mm × mm)	Population (nb of cross-section)
20	125.7	25,148.4	Non uniform	--	--	--	40 × 40	700
			Uniform	40	240	5	40 × 40	700
30	188.5	84,846.6	Non uniform	--	--	--	60 × 60	700
			Uniform	40	400	9	60 × 60	702

[(1)]*: the radius is measured at the neutral axis of the wall thickness*

The average errors, over 10 runs, in cross-sectional area and second moments of area are given in Table 14. The distribution type has little influence on the accuracy of the algorithm with the average error over 10 runs at the 100th generation being similar for uniformly and non-uniformly distributed initial populations. Yet, for the 30 mm radius circle, the algorithm converges faster to the optimum solution for the uniformly distributed initial population than for the non-uniformly distributed, as shown in Figure 19. Consequently, to allow diversity within the initial population, a uniform distribution of the cross-sectional areas in the initial population is recommended.

Table 14: Average results at the 100th generation for various distributions of the initial population

	Results over 10 runs at the 100th generation					
	A_s		I_{sx}		I_{sy}	
Optimum radius (mm)	Aver. error (%)	CoV	Aver. error (%)	CoV	Aver. error (%)	CoV
20 (non uniform distribution)	0.36	0.0016	0.02	0.0001	0.04	0.0005
20 (uniform distribution)	0.30	0.0015	0.02	0.0002	0.04	0.0005
30 (non uniform distribution)	0.82	0.0020	0.06	0.0005	0.05	0.0004
30 (uniform distribution)	0.87	0.0030	0.04	0.0006	0.04	0.0004

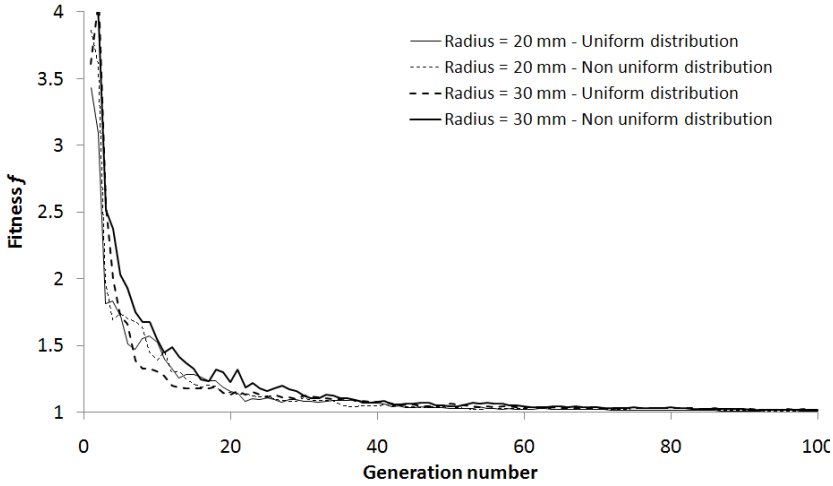

Figure 19: Average fitness f for various distribution and circle radii

5 DISCUSION AND FUTURE WORK

As a case study, the self-shape optimisation process described in the report will be extended and applied to investigate new cross-sectional shapes of cold-formed steel storage rack uprights by introducing manufacturing and storage rack specific constraints. The aim is to find practical cross-sections which perform better than existing ones.

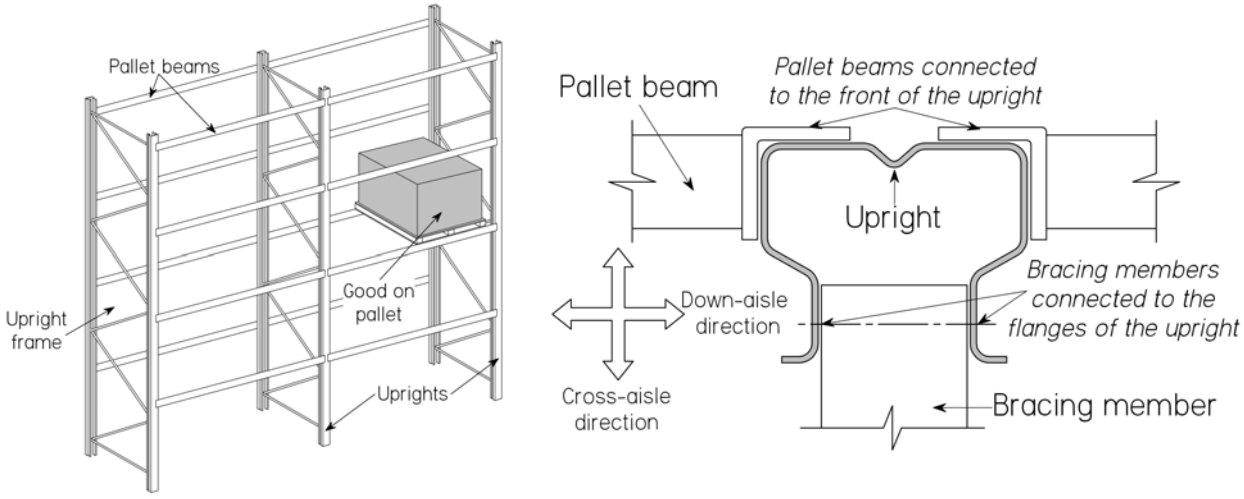

(a) *(b)*

Figure 20: (a) general lay-out of steel storage rack upright and (b) upright cross-section showing bracing and pallet beam member connections

5.1 Manufacturing challenges

In storage racks, uprights are open sections connected in one direction (cross-aisle) by bracing members which are inserted between the flanges of the uprights, forming an "upright frame". In the other direction (down-aisle), upright frames are linked together by pallet beams which are inserted into perforations in the upright web [29], see Figure 20. These features, specific to current practices, will be introduced into the optimisation process with the cross-section allowing space to connect bracing members and pallet beams. New inequalities constraints could be introduced in the fitness function *f* in Eq. (2) to penalise cross-sections which do not have sufficient space to insert bracing members and pallet beams, alternatively parts of the cross-sections may be predrawn at specific locations so to allow connections.

5.2 Design and computation time challenges

In Australia, cold-formed steel structures can be designed using two distinct methods specified in the cold-formed steel standard AS 4600 [30], referred to as the "effective width method" and the "Direct Strength Method" (DSM). The DSM allows any cross-section to be designed with the same degree of complexity whereas unusual cross-sections lead to cumbersome calculations using the effective width method [31]. Therefore, the DSM is well adapted to the self-shape optimisation principle and evaluates the strength to weight ratio of arbitrarily drawn cross-sections. The finite strip method is intended to be linked to the GA and the DSM to determine local, distortional and overall elastic buckling loads.

As studied in Section 4.2, the computational time required to find an optimum cross-section of about 30 elements is equal to 0.65 hour per run on a 3 GHz Intel Core2 Quad processor, 11.3 less than for an optimum cross-section of about 60 elements. Therefore, a large number of elements leads to unsatisfactory computational time and keeping the number of elements constituting the cross-section of about 30 seems to be a reasonable choice in the present study.

Steel storage rack uprights are singly symmetric profiles and only half of the cross-section needs to be modelled in the optimisation process. Figure 21 shows a typical, 2 mm thick and 90 mm wide, cross-section currently used in industry and the same cross-section drawn with 33 elements of about 4 mm. Dimensions and main section properties of the cross-sections are given in Appendix 8. The cross-sectional area of the actual cross-section is equal to 526.3 mm^2 whereas the cross-sectional area of the simplified cross-section in Figure 21 is equal to 515.9 mm^2, i.e. a difference between the two cross-sectional areas less than 2%.

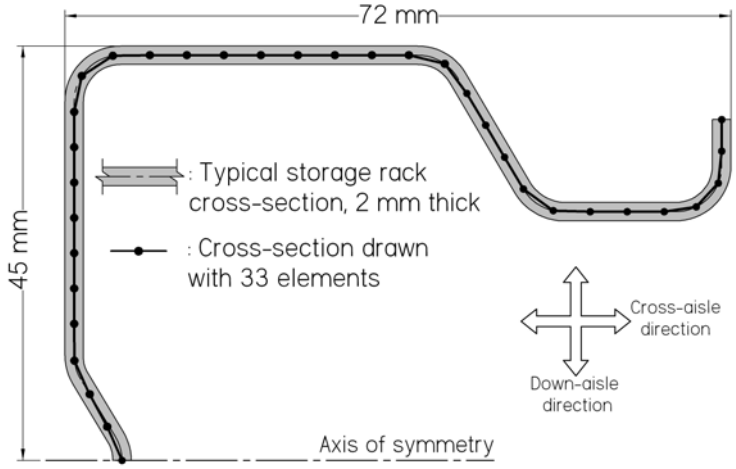

Figure 21: Current upright drawn with 33 elements

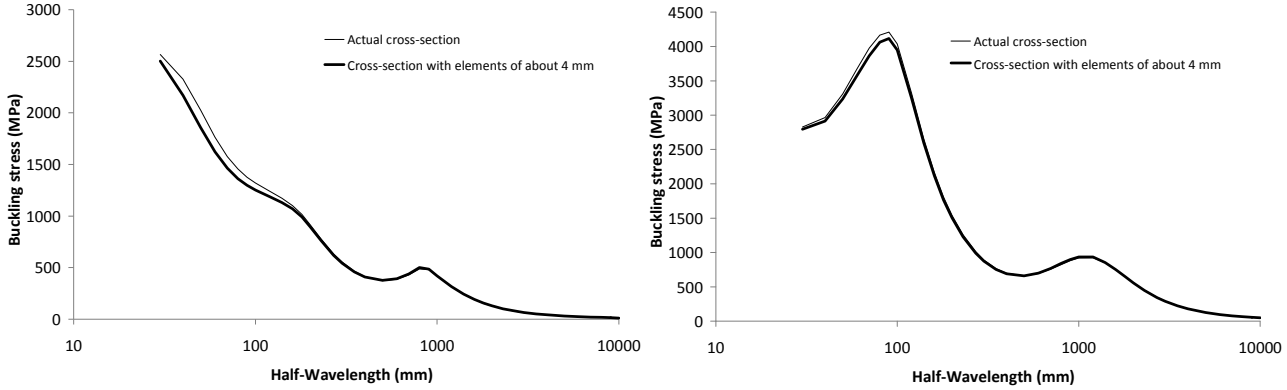

(a) *(b)*

Figure 22: Buckling curves for the actual and simplified cross-sections (a) compression and (b) bending about the major axis of bending

Figure 22 plots the buckling curves in compression and bending about the major axis of bending (axis of symmetry of the cross-section) for the actual and simplified cross-sections using the software Thin-Wall [32]. The local, distortional and overall buckling loads are summarised in Table 15. The differences in buckling stresses between the actual and simplified cross-sections is found to be less than 1% for the distortional and overall buckling modes and less than 5% for the local buckling mode, with the local buckling stress being higher than the yield stress, as shown in Table 15.

Table 15: Elastic buckling loads for a typical 90 mm wide storage rack cross-section

	Compression			Bending		
	Local (MPa)[(1)]	Distortional (MPa)	Overall (MPa)[(2)]	Local (MPa)[(2)]	Distortional (MPa)	Overall (MPa)[(2)]
Actual cross-section	1240	375	128	3315	661	559
Simplified cross-section	1186	376	129	3243	663	557
Difference (%)	*4.4*	*0.3*	*0.8*	*2.2*	*0.3*	*0.4*

[(1)]: taken at a half-wavelength of 120 mm
[(2)]: taken at a half-wavelength of 2000 mm

Consequently, choosing an element size of twice the thickness profile seems to be a reasonable choice in terms of both accuracy and computational time, for further studies. This choice allows internal bending radii of 0.91 times the profile thickness, for a 90° bend, to be drawn in the initial population (see Figure 23 (a)), in the order of magnitude of the minimum bending radius specified in the EN 10149-2 [33] for plates less than 3 mm thick.

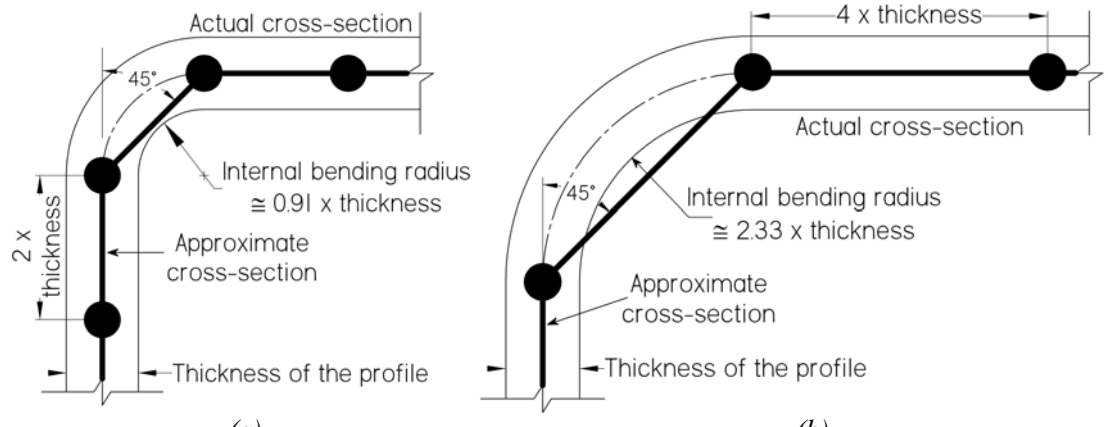

(a) *(b)*

Figure 23: Minimum Internal bending radius for a 90° bend in the initial population

Moreover, to further reduce computational time, an element size of four times the profile thickness would allow internal bending radii of 2.33 times the profile thickness, for a 90° bend, to be drawn in the initial population (see Figure 23 (b)). This value is still reasonable and is about twice higher than the minimum bending radius specified in the EN 10149-2 [33] for plates less than 3 mm thick.

6 CONCLUSIONS

This report introduced the concept of a new optimisation procedure which allows arbitrary and continuously drawn cross-sections to self-shape to an optimum by using Genetic Algorithm and the Augmented Lagragian method. The cross-over and mutation operators are described. The proposed method is checked against known solutions of minimising the cross-sectional area of thin-walled closed profiles for given second moments of area and is found to accurately converge to these solutions. Future challenges of applying the method to find new cold-formed steel profiles with practical applications are discussed in terms of constraints, computational time and accuracy.

7 REFERENCES

[1] G.J. Hancock, *Design of cold-formed steel structures (to AS/NZ 4600:2007) - 4th Edition*, (Australian Steel Institute), North Sydney, Australia, 2007.

[2] M. Ostwald, M. Rodak, "Multicriteria optimisation of cold-formed thin-walled beams under compression axial load", *Proceedings of the 5th International Conference on Coupled Instabilities in Metal Structures* (Eds.: K.J.R. Rasmussen, T. Wilkinson), Sydney, Australia, 141-148, 2008.

[3] R.J. Kasperska, K. Magnucki, M. Ostwald "Bicriteria optimization of cold-formed thin-walled beams with monosymmetrical open cross sections under pure bending", *Thin-Walled Structures*, 45, 563-572, 2007.

[4] K. Magnucki, P. Paczos "Theoretical shape optimization of cold-formed thin-walled channel beams with drop flanges in pure bending", *Journal of Constructional Steel Research*, 65, 1731-1737, 2009.

[5] K. Magnucki, M. Mackiewicz, J. Lewinski "Optimal design of a mono-symmetrical open cross section of a cold-formed beam with cosinusoidally corrugated flanges", *Thin-Walled Structures*, 44, 554-562, 2006.

[6] J. Lee, S.-M. Kim, H.-S. Park, B.-H. Woo "Optimum design of cold-formed steel channel beams using micro Genetic Algorithm", *Engineering Structures*, 27, 17-24, 2005.

[7] J. Lee, S.-M. Kim, H. Seon Park "Optimum design of cold-formed steel columns by using micro genetic algorithms", *Thin-Walled Structures*, 44, 952-960, 2006.

[8] A. Karim, H. Adeli "Global optimum design of cold-formed steel hat-shape beams", *Thin-Walled Structures*, 35, 275-288, 1999.

[9] M.M. Pastor, M. Casafont, E. Chillarón, A. Lusa, F. Roure, M.R. Somalo "Optimization of cold-formed steel pallet racking cross-sections for flexural-torsional buckling with constraints on the geometry", *Engineering Structures*, 31, 2711-2722, 2009.

[10] D.R. Griffiths, J.C. Miles "Determining the optimal cross-section of beams", *Advanced Engineering Informatics*, 17, 59-76, 2003.

[11] J. Holland, *Adaptation in Natural and Artificial Systems*, (University of Michigan Press, Ann Arbor), 1975.

[12] M. Gen, R. Cheng, *Genetic algorithms and engineering design*, New York, 1997.

[13] R. Haupt, S. Haupt, *Practical genetic algorithms*, New York, 1998.

[14] T. Xu, W. Zuo, T. Xu, G. Song, R. Li "An adaptive reanalysis method for genetic algortihm with application to fast truss optimization", *Acta Mechanica Sinica* 26, 225-234, 2010.

[15] N. Bel Hadj Ali, M. Sellami, A.-F. Cutting-Decelle, J.-C. Mangin "Multi-stage production cost optimization of semi-rigid steel frames using genetic algorithms", *Engineering Structures*, 31, 2766-2778, 2009.

[16] M.N.S. Hadi, Y. Arfiadi "Optimum design of absorber for MDOF structures", *Journal of Structural Engineering - ASCE*, 124, 1272-1280, 1998.

[17] A.M. El Ansary, A.A. El Damatty, A.O. Nassef "A coupled finite element genetic algorithm technique for optimum design of steel conical tanks", *Thin-Walled Structures*, 48, 260-273, 2010.

[18] Z. Aydin, Y. Ayvaz "Optimum topology and shape design of prestressed concrete bridge girders using a genetic algortihm", *Structural and Multidisciplinary Optimization*, 41, 151-162, 2010.

[19] W. Lu, P. Makelainen, "Augmented Lagrangian genetic algorithms for optimal design of hat-shaped cold-formed steel profile", *Proceedings of the 9th International Conference: Modern Building Materials, Structures and Techniques*, Vilnius, Lithuania, 2007.

[20] W. Lu, P. Mäkeläinen "Fuzzy optimization of cold-formed steel sheeting using genetic algorithms", *Journal of Constructional Steel Research*, 62, 1276-1281, 2006.

[21] W. Lu, *Optimum design of cold-formed steel purlins using genetic algorithms* PhD Thesis, Helsinki University of Technology, Helsinki, Finland, 2006.

[22] H. Liu, T. Igusa, B.W. Schafer "Knowledge-based global optimization of cold-formed steel columns", *Thin-Walled Structures*, 42, 785-801, 2004.

[23] J. Leng, J.K. Guest, B.W. Schafer "Shape optimization of cold-formed steel columns", *Thin-Walled Structures*, 49, 1492-1503, 2011.

[24] F. Ragnedda, M. Serra "On optimum thin-walled closed cross section ", *Structural and Multidisciplinary Optimization*, 30, 233-235, 2005.

[25] H. Adeli, C.S. Kamal, *Cost optimization of structures*, (Wiley), Chichester, England, 2006.

[26] H. Adeli, N.-T. Cheng "Augmented Lagrangian Genetic Algorithm for Structural Optimization", *Journal of Aerospace Engineering*, 7, 104-118, 1994.

[27] A.D. Belegundu, J.S. Arora "A computational study of transformation methods for optimal design", *American Institute of Aeronautics and Astronautics Journal*, 22, 535-542, 1984.

[28] M.S. Bazaraa, H.D. Sherali, C.M. Shetty, *Nonlinear programming, theory and algorithms, second edition*, (Wiley & Sons), New-York, USA, 1993.

[29] F.D. Markazi, R.G. Beale, M.H.R. Godley "Experimental analysis of semi-rigid boltless connectors", *Thin-Walled Structures*, 28, 57-87, 1997.

[30] AS/NZS 4600, *Cold-formed steel structures*, Standards Australia, Sydney, Australia, 2005.

[31] B.W. Schafer, "Designing cold-formed steel using the direct strength method", *Proceedings of the 18th International Specialty Conference on Cold-Formed Steel Structures* (Eds.: R.A. LaBoule, W.W. Yu), Orlando, Florida, 2006.

[32] Thin-Wall, *Thin-Wall ver. 2.1.33 - User manual*, (Centre for Advanced Structural Engineering, The University of Sydney), Sydney, Australia, 2011.

[33] EN 10149-2, *Specification for hot-rolled flat products made of high yield strength steels for cold forming. Delivery conditions for thermomechanically rolled steels*, European Committee for Standardization (CEN), Brussels, Belgium, 1996.

Appendix 1

Detailed results on the influence of the population size

Size of the lattice		
Maximum lattice size in x =	40	points
Maximum lattice size in y =	40	points
Maximum lattice size in x =	40	mm
Maximum lattice size in y =	40	mm
Targeted profile		
Thickness =	1	mm
Second moment of area about x =	25148.4	mm4
Second moment of area about y =	25148.4	mm4
Optimum radius on the lattice in x =	20	mm
Optimum radius on the lattice in y =	20	mm
Optimum area on the lattice =	125.664	mm2
Parameters for the first generation of parents		
The initial generation is uniformly distributed		
Minimum number of points per parent =	10	
Maximum number of points per parent =	60	
Number of points per category =	10	
Number of parents per category =	N/A	
Total number of individuals =	N/A	
Total number of individuals in the mating pool =	N/A	
GA parameters		
Maximum number of generations =	100	
Cross-over probability =	0.8	
Mutation probability =	0.01	
Maximum of the individual length to be mutated if mutation occurs =	50	%
Augmented Lagrangian parameters		
Initial Gamma1 =	2	
Initial Gamma2 =	2	
Initial Mu1 =	0	
Initial Mu2 =	0	
Alpha =	1.5	
Beta =	1.05	

Results

Number of parents per category =	Run 1			Run 2			Run 3			Run 4			Run 5		
	Area mm2	Ix mm4	Iy mm4	Area mm2	Ix mm4	Iy mm4	Area mm2	Ix mm4	Iy mm4	Area mm2	Ix mm4	Iy mm4	Area mm2	Ix mm4	Iy mm4
140	126.0237	25150.21	25145.65	125.9059	25135.14	25127.1	125.9492	25131.21	25145.81	126.3833	25136.69	25112.17	126.1398	25144.99	25148.37
80	126.2844	25154.65	25148.77	126.0328	25151.15	25146.14	126.5201	25150.87	25145.15	126.1695	25127.48	25153.56	126.1136	25145.3	25148.47
200	125.9923	25157.72	25146.33	125.9734	25143.86	25151.65	126.0041	25141.36	25148.4	126.0715	25140.57	25146.31	125.8569	25134.08	25146.14
	Run 6			Run 7			Run 8			Run 9			Run 10		
	Area mm2	Ix mm4	Iy mm4	Area mm2	Ix mm4	Iy mm4	Area mm2	Ix mm4	Iy mm4	Area mm2	Ix mm4	Iy mm4	Area mm2	Ix mm4	Iy mm4
140	125.9576	25141.15	25143.53	125.8852	25152.6	25132.04	126.3329	25148.91	25167.02	125.9297	25148.29	25148.07	125.8917	25148.91	25149.89
80	126.1498	25141.21	25149.11	126.8802	25148.64	25148.66	126.573	25148.78	25146.72	125.9759	25143.65	25149.79	126.1708	25147.75	25159.51
200	125.9491	25145.85	25149.46	125.948	25149.65	25145.65	126.0399	25148.91	25139.88	125.9145	25145.29	25138.69	126.0095	25146.36	25154.69

Difference relative to optimum

Number of parents per category =	Run 1			Run 2			Run 3			Run 4			Run 5		
	Area %	Ix %	Iy %	Area %	Ix %	Iy %	Area %	Ix %	Iy %	Area %	Ix %	Iy %	Area %	Ix %	Iy %
140	0.29	0.01	0.01	0.19	0.05	0.08	0.23	0.07	0.01	0.57	0.05	0.14	0.38	0.01	0.00
80	0.49	0.02	0.00	0.29	0.01	0.01	0.68	0.01	0.01	0.40	0.08	0.02	0.36	0.01	0.00
200	0.26	0.04	0.01	0.25	0.02	0.01	0.27	0.03	0.00	0.32	0.03	0.01	0.15	0.06	0.01
	Run 6			Run 7			Run 8			Run 9			Run 10		
	Area %	Ix %	Iy %	Area %	Ix %	Iy %	Area %	Ix %	Iy %	Area %	Ix %	Iy %	Area %	Ix %	Iy %
140	0.23	0.03	0.02	0.18	0.02	0.07	0.53	0.00	0.07	0.21	0.00	0.00	0.18	0.00	0.01
80	0.39	0.03	0.00	0.97	0.00	0.00	0.72	0.00	0.01	0.25	0.02	0.01	0.40	0.00	0.04
200	0.23	0.01	0.00	0.23	0.00	0.01	0.30	0.00	0.03	0.20	0.01	0.04	0.27	0.01	0.03

Number of parents per category =	Average			Standard deviation			Minimum			Maximum		
	Area %	Ix %	Iy %	Area %	Ix %	Iy %	Area %	Ix %	Iy %	Area %	Ix %	Iy %
140	0.30	0.02	0.04	0.15	0.02	0.05	0.18	0.00	0.00	0.57	0.07	0.14
80	0.50	0.02	0.01	0.23	0.02	0.01	0.25	0.00	0.00	0.97	0.08	0.04
200	0.25	0.02	0.02	0.05	0.02	0.01	0.15	0.00	0.00	0.32	0.06	0.04

Appendix 2

Detailed results on the influence of the maximum mutation length

Size of the lattice		
Maximum lattice size in x =	40	points
Maximum lattice size in y =	40	points
Maximum lattice size in x =	40	mm
Maximum lattice size in y =	40	mm
Targeted profile		
Thickness =	1	mm
Second moment of area about x =	25148.4	mm4
Second moment of area about y =	25148.4	mm4
Optimum radius on the lattice in x =	20	mm
Optimum radius on the lattice in y =	20	mm
Optimum area on the lattice =	125.664	mm2
Parameters for the first generation of parents		
The initial generation is uniformly distributed		
Minimum number of points per parent =	10	
Maximum number of points per parent =	60	
Number of points per category =	10	
Number of parents per category =	140	
Total number of individuals =	700	
Total number of individuals in the mating pool =	350	
GA parameters		
Maximum number of generations =	100	
Cross-over probability =	0.8	
Mutation probability =	0.01	
Maximum of the individual length to be mutated if mutation occurs =	N/A	%
Augmented Lagrangian parameters		
Initial Gamma1 =	2	
Initial Gamma2 =	2	
Initial Mu1 =	0	
Initial Mu2 =	0	
Alpha =	1.5	
Beta =	1.05	

Results

Max mutated length =	Run 1			Run 2			Run 3			Run 4			Run 5		
	Area mm2	Ix mm4	Iy mm4	Area mm2	Ix mm4	Iy mm4	Area mm2	Ix mm4	Iy mm4	Area mm2	Ix mm4	Iy mm4	Area mm2	Ix mm4	Iy mm4
30	125.8106	25147.46	25146.12	125.8403	25140.13	25142.88	126.0926	25147.78	25147.91	126.137	25147.37	25142.55	125.9242	25140.48	25148.85
70	125.792	25144.96	25144.65	126.1478	25154.85	25143.18	125.9937	25130.25	25141.16	126.1763	25136.11	25150.01	126.2846	25138.8	25157.47
50	126.0237	25150.21	25145.65	125.9059	25135.14	25127.1	125.9492	25131.21	25145.81	126.3833	25136.69	25112.17	126.1398	25144.99	25148.37
	Run 6			Run 7			Run 8			Run 9			Run 10		
	Area mm2	Ix mm4	Iy mm4	Area mm2	Ix mm4	Iy mm4	Area mm2	Ix mm4	Iy mm4	Area mm2	Ix mm4	Iy mm4	Area mm2	Ix mm4	Iy mm4
30	126.4236	25141.45	25140.29	125.8583	25154.9	25148.92	126.3114	25117.9	25158.44	126.1017	25150.44	25155.69	125.8552	25147.51	25139.07
70	125.8212	25134.83	25135.33	126.0504	25148.18	25140.9	125.9521	25158	25137.66	126.1704	25153.98	25141.16	125.9201	25137.78	25137.63
50	125.9576	25141.15	25143.53	125.8852	25152.6	25132.04	126.3329	25148.91	25167.02	125.9297	25148.29	25148.07	125.8917	25148.91	25149.89

Difference relative to optimum

Max mutated length =	Run 1			Run 2			Run 3			Run 4			Run 5		
	Area %	Ix %	Iy %	Area %	Ix %	Iy %	Area %	Ix %	Iy %	Area %	Ix %	Iy %	Area %	Ix %	Iy %
30	0.12	0.00	0.01	0.14	0.03	0.02	0.34	0.00	0.00	0.38	0.00	0.02	0.21	0.03	0.00
70	0.10	0.01	0.01	0.38	0.03	0.02	0.26	0.07	0.03	0.41	0.05	0.01	0.49	0.04	0.04
50	0.29	0.01	0.01	0.19	0.05	0.08	0.23	0.07	0.01	0.57	0.05	0.14	0.38	0.01	0.00
	Run 6			Run 7			Run 8			Run 9			Run 10		
	Area %	Ix %	Iy %	Area %	Ix %	Iy %	Area %	Ix %	Iy %	Area %	Ix %	Iy %	Area %	Ix %	Iy %
30	0.60	0.03	0.03	0.15	0.03	0.00	0.52	0.12	0.04	0.35	0.01	0.03	0.15	0.00	0.04
70	0.13	0.05	0.05	0.31	0.00	0.03	0.23	0.04	0.04	0.40	0.02	0.03	0.20	0.04	0.04
50	0.23	0.03	0.02	0.18	0.02	0.07	0.53	0.00	0.07	0.21	0.00	0.00	0.18	0.00	0.01

Max mutated length =	Average			Standard deviation			Minimum			Maximum		
	Area %	Ix %	Iy %	Area %	Ix %	Iy %	Area %	Ix %	Iy %	Area %	Ix %	Iy %
30	0.30	0.03	0.02	0.17	0.04	0.02	0.12	0.00	0.00	0.60	0.12	0.04
70	0.29	0.04	0.03	0.13	0.02	0.01	0.10	0.00	0.01	0.49	0.07	0.05
50	0.30	0.02	0.04	0.15	0.02	0.05	0.18	0.00	0.00	0.57	0.07	0.14

Appendix 3

Detailed results on the influence of the penalty increasing constant β

Size of the lattice		
Maximum lattice size in x =	40	points
Maximum lattice size in y =	40	points
Maximum lattice size in x =	40	mm
Maximum lattice size in y =	40	mm
Targeted profile		
Thickness =	1	mm
Second moment of area about x =	25148.4	mm4
Second moment of area about y =	25148.4	mm4
Optimum radius on the lattice in x =	20	mm
Optimum radius on the lattice in y =	20	mm
Optimum area on the lattice =	125.664	mm2
Parameters for the first generation of parents		
The initial generation is uniformly distributed		
Minimum number of points per parent =	10	
Maximum number of points per parent =	60	
Number of points per category =	10	
Number of parents per category =	140	
Total number of individuals =	700	
Total number of individuals in the mating pool =	350	
GA parameters		
Maximum number of generations =	100	
Cross-over probability =	0.8	
Mutation probability =	0.01	
Maximum of the individual length to be mutated if mutation occurs =	50	%
Augmented Lagrangian parameters		
Initial Gamma1 =	2	
Initial Gamma2 =	2	
Initial Mu1 =	0	
Initial Mu2 =	0	
Alpha =	1.5	
Beta =	N/A	

Results

Beta factor =	Run 1			Run 2			Run 3			Run 4			Run 5		
	Area mm2	Ix mm4	Iy mm4	Area mm2	Ix mm4	Iy mm4	Area mm2	Ix mm4	Iy mm4	Area mm2	Ix mm4	Iy mm4	Area mm2	Ix mm4	Iy mm4
10	132.9697	25148.42	25148.42	140.716	25148.4	25148.4	140.7901	25148.4	25148.39	139.7381	25148.38	25148.41	136.0178	25148.41	25148.4
1.01	126.4499	25146.65	25153.69	125.9122	25153.4	25145.05	125.868	25149.02	25127.37	126.0054	25151.04	25126.49	126.1312	25123.62	25143.92
1.1	126.0762	25152.38	25134.94	126.3439	25135.81	25149.14	126.1476	25131.32	25147.72	126.2206	25140.85	25148.24	126.1357	25139.8	25149.06
1.5	128.9214	25148.4	25148.4	130.9619	25148.4	25148.4	129.7787	25148.37	25148.4	130.3318	25148.4	25148.41	128.2268	25148.4	25148.39
2	131.1565	25148.4	25148.4	132.0414	25148.4	25148.4	135.2064	25148.4	25148.4	130.9101	25148.4	25148.4	129.775	25148.4	25148.4
1.05	126.0237	25150.21	25145.65	125.9059	25135.14	25127.1	125.9492	25131.21	25145.81	126.3833	25136.69	25112.17	126.1398	25144.99	25148.37
	Run 6			Run 7			Run 8			Run 9			Run 10		
	Area mm2	Ix mm4	Iy mm4	Area mm2	Ix mm4	Iy mm4	Area mm2	Ix mm4	Iy mm4	Area mm2	Ix mm4	Iy mm4	Area mm2	Ix mm4	Iy mm4
10	132.7542	25148.41	25148.42	135.6248	25148.41	25148.38	133.8439	25148.41	25148.38	139.6614	25148.4	25148.42	136.8487	25148.4	25148.4
1.01	125.8406	25067.46	25136.01	125.7815	25131.25	25148.96	126.3834	25149.75	25145.08	126.0199	25151.77	25049.91	126.1441	25153.01	25152.11
1.1	126.1442	25151.8	25145.77	126.2568	25144.23	25149.55	125.9761	25140.33	25148.65	127.6531	25148.21	25145.1	126.1267	25155.54	25143.74
1.5	128.9938	25148.39	25148.36	129.1026	25148.4	25148.43	129.6281	25148.4	25148.4	128.6769	25148.4	25148.37	129.5261	25148.4	25148.4
2	128.7901	25148.4	25148.4	133.61	25148.4	25148.4	130.2518	25148.4	25148.4	130.925	25148.4	25148.4	129.6486	25148.4	25148.4
1.05	125.9576	25141.15	25143.53	125.8852	25152.6	25132.04	126.3329	25148.91	25167.02	125.9297	25148.29	25148.07	125.8917	25148.91	25149.89

Difference relative to optimum

Beta factor =	Run 1			Run 2			Run 3			Run 4			Run 5		
	Area %	Ix %	Iy %	Area %	Ix %	Iy %	Area %	Ix %	Iy %	Area %	Ix %	Iy %	Area %	Ix %	Iy %
10	5.81	0.00	0.00	11.98	0.00	0.00	12.04	0.00	0.00	11.20	0.00	0.00	8.24	0.00	0.00
1.01	0.63	0.01	0.02	0.20	0.02	0.01	0.16	0.00	0.08	0.27	0.01	0.09	0.37	0.10	0.02
1.1	0.33	0.02	0.05	0.54	0.05	0.00	0.38	0.07	0.00	0.44	0.03	0.00	0.38	0.03	0.00
1.5	2.59	0.00	0.00	4.22	0.00	0.00	3.27	0.00	0.00	3.71	0.00	0.00	2.04	0.00	0.00
2	4.37	0.00	0.00	5.07	0.00	0.00	7.59	0.00	0.00	4.17	0.00	0.00	3.27	0.00	0.00
1.05	0.29	0.01	0.01	0.19	0.05	0.08	0.23	0.07	0.01	0.57	0.05	0.14	0.38	0.01	0.00
	Run 6			Run 7			Run 8			Run 9			Run 10		
	Area %	Ix %	Iy %	Area %	Ix %	Iy %	Area %	Ix %	Iy %	Area %	Ix %	Iy %	Area %	Ix %	Iy %
10	5.64	0.00	0.00	7.93	0.00	0.00	6.51	0.00	0.00	11.14	0.00	0.00	8.90	0.00	0.00
1.01	0.14	0.32	0.05	0.09	0.07	0.00	0.57	0.01	0.01	0.28	0.01	0.39	0.38	0.02	0.01
1.1	0.38	0.01	0.01	0.47	0.02	0.00	0.25	0.03	0.00	1.58	0.00	0.01	0.37	0.03	0.02
1.5	2.65	0.00	0.00	2.74	0.00	0.00	3.15	0.00	0.00	2.40	0.00	0.00	3.07	0.00	0.00
2	2.49	0.00	0.00	6.32	0.00	0.00	3.65	0.00	0.00	4.19	0.00	0.00	3.17	0.00	0.00
1.05	0.23	0.03	0.02	0.18	0.02	0.07	0.53	0.00	0.07	0.21	0.00	0.00	0.18	0.00	0.01

Beta factor =	Average			Standard deviation			Minimum			Maximum		
	Area %	Ix %	Iy %	Area %	Ix %	Iy %	Area %	Ix %	Iy %	Area %	Ix %	Iy %
10	8.94	0.00	0.00	2.51	0.00	0.00	5.64	0.00	0.00	12.04	0.00	0.00
1.01	0.31	0.06	0.07	0.18	0.10	0.12	0.09	0.00	0.00	0.63	0.32	0.39
1.1	0.51	0.03	0.01	0.38	0.02	0.02	0.25	0.00	0.00	1.58	0.07	0.05
1.5	2.98	0.00	0.00	0.64	0.00	0.00	2.04	0.00	0.00	4.22	0.00	0.00
2	4.43	0.00	0.00	1.54	0.00	0.00	2.49	0.00	0.00	7.59	0.00	0.00
1.05	0.30	0.02	0.04	0.15	0.02	0.05	0.18	0.00	0.00	0.57	0.07	0.14

Appendix 4

Detailed results on the influence of the penalty function coefficients

Size of the lattice		
Maximum lattice size in x =	40	points
Maximum lattice size in y =	40	points
Maximum lattice size in x =	40	mm
Maximum lattice size in y =	40	mm
Targeted profile		
Thickness =	1	mm
Second moment of area about x =	25148.4	mm4
Second moment of area about y =	25148.4	mm4
Optimum radius on the lattice in x =	20	mm
Optimum radius on the lattice in y =	20	mm
Optimum area on the lattice =	125.664	mm2
Parameters for the first generation of parents		
The initial generation is uniformly distributed		
Minimum number of points per parent =	10	
Maximum number of points per parent =	60	
Number of points per category =	10	
Number of parents per category =	140	
Total number of individuals =	700	
Total number of individuals in the mating pool =	350	
GA parameters		
Maximum number of generations =	100	
Cross-over probability =	0.8	
Mutation probability =	0.01	
Maximum of the individual length to be mutated if mutation occurs =	50	%
Augmented Lagrangian parameters		
Initial Gamma1 =	N/A	
Initial Gamma2 =	N/A	
Initial Mu1 =	0	
Initial Mu2 =	0	
Alpha =	1.5	
Beta =	1.05	

Results

Gamma factor =	Run 1			Run 2			Run 3			Run 4			Run 5		
	Area mm2	Ix mm4	Iy mm4	Area mm2	Ix mm4	Iy mm4	Area mm2	Ix mm4	Iy mm4	Area mm2	Ix mm4	Iy mm4	Area mm2	Ix mm4	Iy mm4
0.5	125.979	25148.69	25143.73	126.0754	25150.18	25151.69	125.9228	25161.68	25151.62	126.0583	25145.62	25149.06	125.8994	25157.41	25149.78
1	125.8081	25152.48	25143.82	125.914	25149.5	25148.73	125.9895	25148.36	25148.03	125.775	25144.1	25143.14	126.3194	25149.4	25137.91
5	126.3594	25137.33	25159.59	126.2179	25154.9	25146.85	125.9915	25135.66	25148.62	126.2283	25153.04	25159.47	126.4066	25134.98	25148.47
2	126.0237	25150.21	25145.65	125.9059	25135.14	25127.1	125.9492	25131.21	25145.81	126.3833	25136.69	25112.17	126.1398	25144.99	25148.37
0.35	125.8613	25152.76	25143.38	125.9341	25138.3	25152.12	126.2102	25148.05	25147.29	125.9271	25154.94	25144.43	125.8836	25147.56	25149.18
	Run 6			Run 7			Run 8			Run 9			Run 10		
	Area mm2	Ix mm4	Iy mm4	Area mm2	Ix mm4	Iy mm4	Area mm2	Ix mm4	Iy mm4	Area mm2	Ix mm4	Iy mm4	Area mm2	Ix mm4	Iy mm4
0.5	125.8205	25150.26	25151.28	125.9623	25154.26	25144.73	126.4113	25147.3	25135.88	125.9172	25144.41	25143.23	126.4307	25147.61	25153.38
1	126.1122	25139.01	25147.15	125.9628	25144.88	25149.22	125.8863	25146.38	25161.04	125.8927	25148.02	25148.63	125.814	25151.47	25147.09
5	126.5347	25153.75	25152.44	126.571	25154.89	25139.3	126.251	25141.17	25155.5	126.2438	25147.83	25150.24	126.0563	25147.34	25149.38
2	125.9576	25141.15	25143.53	125.8852	25152.6	25132.04	126.3329	25148.91	25167.02	125.9297	25148.29	25148.07	125.8917	25148.91	25149.89
0.35	125.9153	25149.44	25132.06	126.0625	25153.77	25142.86	126.2157	25152.21	25141.78	125.9441	25148.54	25158	126.0751	25149.16	25157.89

Difference relative to optimum

Gamma factor =	Run 1			Run 2			Run 3			Run 4			Run 5		
	Area %	Ix %	Iy %	Area %	Ix %	Iy %	Area %	Ix %	Iy %	Area %	Ix %	Iy %	Area %	Ix %	Iy %
0.5	0.25	0.00	0.02	0.33	0.01	0.01	0.21	0.05	0.01	0.31	0.01	0.00	0.19	0.04	0.01
1	0.11	0.02	0.02	0.20	0.00	0.00	0.26	0.00	0.00	0.09	0.02	0.02	0.52	0.00	0.04
5	0.55	0.04	0.04	0.44	0.03	0.01	0.26	0.05	0.00	0.45	0.02	0.04	0.59	0.05	0.00
2	0.29	0.01	0.01	0.19	0.05	0.08	0.23	0.07	0.01	0.57	0.05	0.14	0.38	0.01	0.00
0.35	0.16	0.02	0.02	0.21	0.04	0.01	0.43	0.00	0.00	0.21	0.03	0.02	0.17	0.00	0.00
	Run 6			Run 7			Run 8			Run 9			Run 10		
	Area %	Ix %	Iy %	Area %	Ix %	Iy %	Area %	Ix %	Iy %	Area %	Ix %	Iy %	Area %	Ix %	Iy %
0.5	0.12	0.01	0.01	0.24	0.02	0.01	0.59	0.00	0.05	0.20	0.02	0.02	0.61	0.00	0.02
1	0.36	0.04	0.00	0.24	0.01	0.00	0.18	0.01	0.05	0.18	0.00	0.00	0.12	0.01	0.01
5	0.69	0.02	0.02	0.72	0.03	0.04	0.47	0.03	0.03	0.46	0.00	0.01	0.31	0.00	0.00
2	0.23	0.03	0.02	0.18	0.02	0.07	0.53	0.00	0.07	0.21	0.00	0.00	0.18	0.00	0.01
0.35	0.20	0.00	0.06	0.32	0.02	0.02	0.44	0.02	0.03	0.22	0.00	0.04	0.33	0.00	0.04

Gamma factor =	Average			Standard deviation			Minimum			Maximum		
	Area %	Ix %	Iy %	Area %	Ix %	Iy %	Area %	Ix %	Iy %	Area %	Ix %	Iy %
0.5	0.31	0.02	0.02	0.17	0.02	0.01	0.12	0.00	0.00	0.61	0.05	0.05
1	0.23	0.01	0.01	0.13	0.01	0.02	0.09	0.00	0.00	0.52	0.04	0.05
5	0.50	0.03	0.02	0.15	0.02	0.02	0.26	0.00	0.00	0.72	0.05	0.04
2	0.30	0.02	0.04	0.15	0.02	0.05	0.18	0.00	0.00	0.57	0.07	0.14
0.35	0.27	0.01	0.02	0.10	0.01	0.02	0.16	0.00	0.00	0.44	0.04	0.06

Appendix 5

Detailed results on the influence of the circle radius

				r = 10 mm	*r* = 20 mm	*r* = 30 mm	*r* = 40 mm
Size of the lattice							
Maximum lattice size in x =	N/A	mm		20	40	60	80
Maximum lattice size in y =	N/A	mm		20	40	60	80
Targeted profile							
Thickness =	1	mm					
Second moment of area about x =	N/A	mm4		3149.45	201093.3	84846.56	25148.4
Second moment of area about y =	N/A	mm4		3149.45	201093.3	84846.56	25148.4
Optimum radius on the lattice in x =	N/A	mm		10	40	30	20
Optimum radius on the lattice in y =	N/A	mm		10	40	30	20
Optimum area on the lattice =	N/A	mm2		62.832	251.327	188.496	125.664
Parameters for the first generation of parents							
The initial generation is uniformly distributed							
Minimum number of points per parent =	N/A						
Maximum number of points per parent =	N/A						
Number of points per category =	10						
Number of parents per category =	N/A						
Total number of individuals =	N/A						
Total number of individuals in the mating pool =	N/A						
GA parameters							
Maximum number of generations =			100				
Cross-over probability =			0.8				
Mutation probability =			0.01				
Maximum of the individual length to be mutated if mutation occurs =			50	%			
Augmented Lagrangian parameters							
Initial Gamma1 =			2				
Initial Gamma2 =			2				
Initial Mu1 =			0				
Initial Mu2 =			0				
Alpha =			1.5				
Beta =			1.05				

Results

radius =	Run 1			Run 2			Run 3			Run 4			Run 5		
	Area mm2	Ix mm4	Iy mm4	Area mm2	Ix mm4	Iy mm4	Area mm2	Ix mm4	Iy mm4	Area mm2	Ix mm4	Iy mm4	Area mm2	Ix mm4	Iy mm4
10	62.94008	3149.237	3148.269	62.93127	3149.442	3149.12	63.15318	3149.473	3149.147	62.94951	3149.328	3149.482	62.93238	3149.933	3149.416
40	254.6126	201039.3	201203.8	255.0285	201064.3	201054.8	254.5277	201047.1	201028.6	257.2266	201099.2	201084.4	255.4709	201077.8	200857.6
30	189.7499	84818.73	84845.77	190.2558	84849.55	84863.72	190.9708	84772.68	84942.51	189.4742	84841.03	84787.88	189.9889	84825.34	84877.17
20	126.0237	25150.21	25145.65	125.9059	25135.14	25127.1	125.9492	25131.21	25145.81	126.3833	25136.69	25112.17	126.1398	25144.99	25148.37
	Run 6			Run 7			Run 8			Run 9			Run 10		
	Area mm2	Ix mm4	Iy mm4	Area mm2	Ix mm4	Iy mm4	Area mm2	Ix mm4	Iy mm4	Area mm2	Ix mm4	Iy mm4	Area mm2	Ix mm4	Iy mm4
10	63.05082	3149.35	3149.405	62.94116	3149.171	3149.47	62.89944	3149.467	3148.811	62.94701	3149.943	3149.84	63.09182	3149.369	3149.264
40	255.1329	201193.1	201099.8	256.3845	201189	201033	255.4998	201073.7	200894.5	255.5381	201133.3	200575.5	254.8337	201248.2	201016.7
30	189.9961	84837.67	84903.06	190.1513	84858.77	84852.36	189.6676	84876	84850.56	191.2584	84829.39	84850.53	189.8366	84668.55	84805.91
20	125.9576	25141.15	25143.53	125.8852	25152.6	25132.04	126.3329	25148.91	25167.02	125.9297	25148.29	25148.07	125.8917	25148.91	25149.89

Difference relative to optimum

radius =	Run 1			Run 2			Run 3			Run 4			Run 5		
	Area %	Ix %	Iy %	Area %	Ix %	Iy %	Area %	Ix %	Iy %	Area %	Ix %	Iy %	Area %	Ix %	Iy %
10	0.17	0.01	0.04	0.16	0.00	0.01	0.51	0.00	0.01	0.19	0.00	0.00	0.16	0.02	0.00
40	1.31	0.03	0.05	1.47	0.01	0.02	1.27	0.02	0.03	2.35	0.00	0.00	1.65	0.01	0.12
30	0.67	0.03	0.00	0.93	0.00	0.02	1.31	0.09	0.11	0.52	0.01	0.07	0.79	0.03	0.04
20	0.29	0.01	0.01	0.19	0.05	0.08	0.23	0.07	0.01	0.57	0.05	0.14	0.38	0.01	0.00
	Run 6			Run 7			Run 8			Run 9			Run 10		
	Area %	Ix %	Iy %	Area %	Ix %	Iy %	Area %	Ix %	Iy %	Area %	Ix %	Iy %	Area %	Ix %	Iy %
10	0.35	0.00	0.00	0.17	0.01	0.00	0.11	0.00	0.02	0.18	0.02	0.01	0.41	0.00	0.01
40	1.51	0.05	0.00	2.01	0.05	0.03	1.66	0.01	0.10	1.68	0.02	0.26	1.40	0.08	0.04
30	0.80	0.01	0.07	0.88	0.01	0.01	0.62	0.03	0.00	1.47	0.02	0.00	0.71	0.21	0.05
20	0.23	0.03	0.02	0.18	0.02	0.07	0.53	0.00	0.07	0.21	0.00	0.00	0.18	0.00	0.01

radius =	Average			Standard deviation			Minimum			Maximum		
	Area %	Ix %	Iy %	Area %	Ix %	Iy %	Area %	Ix %	Iy %	Area %	Ix %	Iy %
10	0.24	0.01	0.01	0.13	0.01	0.01	0.11	0.00	0.00	0.51	0.02	0.04
40	1.63	0.03	0.07	0.33	0.02	0.08	1.27	0.00	0.00	2.35	0.08	0.26
30	0.87	0.04	0.04	0.30	0.06	0.04	0.52	0.00	0.00	1.47	0.21	0.11
20	0.30	0.02	0.04	0.15	0.02	0.05	0.18	0.00	0.00	0.57	0.07	0.14

Appendix 6

Detailed results on different moments of area about the two main axes of bending

Size of the lattice		
Maximum lattice size in x =	60	points
Maximum lattice size in y =	30	points
Maximum lattice size in x =	40	mm
Maximum lattice size in y =	30	mm
Targeted profile		
Thickness =	1	mm
Second moment of area about x =	18569.76	mm4
Second moment of area about y =	53034.99	mm4
Optimum radius on the lattice in x =	30	mm
Optimum radius on the lattice in y =	15	mm
Optimum area on the lattice =	141.372	mm2
Parameters for the first generation of parents		
The initial generation is uniformly distributed		
Minimum number of points per parent =	10	
Maximum number of points per parent =	60	
Number of points per category =	10	
Number of parents per category =	140	
Total number of individuals =	700	
Total number of individuals in the mating pool =	350	
GA parameters		
Maximum number of generations =	100	
Cross-over probability =	0.8	
Mutation probability =	0.01	
Maximum of the individual length to be mutated if mutation occurs =	50	%
Augmented Lagrangian parameters		
Initial Gamma1 =	2	
Initial Gamma2 =	2	
Initial Mu1 =	0	
Initial Mu2 =	0	
Alpha =	1.5	
Beta =	1.05	

Results

	Run 1			Run 2			Run 3			Run 4			Run 5		
	Area mm2	Ix mm4	Iy mm4	Area mm2	Ix mm4	Iy mm4	Area mm2	Ix mm4	Iy mm4	Area mm2	Ix mm4	Iy mm4	Area mm2	Ix mm4	Iy mm4
	144.3664	18564.39	53040.36	143.9994	18562.2	52932.68	144.5012	18558.95	53033.52	144.0865	18560.51	53010.67	144.5113	18570.15	53024.47
	Run 6			Run 7			Run 8			Run 9			Run 10		
	Area mm2	Ix mm4	Iy mm4	Area mm2	Ix mm4	Iy mm4	Area mm2	Ix mm4	Iy mm4	Area mm2	Ix mm4	Iy mm4	Area mm2	Ix mm4	Iy mm4
	144.2537	18573.05	52994.33	144.6957	18555.13	52981.14	144.2032	18575.57	53020.04	144.5177	18574.9	52975.84	144.0016	18574.41	52982.81

Difference relative to optimum

	Run 1			Run 2			Run 3			Run 4			Run 5		
	Area %	Ix %	Iy %	Area %	Ix %	Iy %	Area %	Ix %	Iy %	Area %	Ix %	Iy %	Area %	Ix %	Iy %
	2.12	0.03	0.01	1.86	0.04	0.19	2.21	0.06	0.00	1.92	0.05	0.05	2.22	0.00	0.02
	Run 6			Run 7			Run 8			Run 9			Run 10		
	Area %	Ix %	Iy %	Area %	Ix %	Iy %	Area %	Ix %	Iy %	Area %	Ix %	Iy %	Area %	Ix %	Iy %
	2.04	0.02	0.08	2.35	0.08	0.10	2.00	0.03	0.03	2.23	0.03	0.11	1.86	0.03	0.10

	Average			Standard deviation			Minimum			Maximum		
	Area %	Ix %	Iy %	Area %	Ix %	Iy %	Area %	Ix %	Iy %	Area %	Ix %	Iy %
	2.08	0.04	0.07	0.17	0.02	0.06	1.86	0.00	0.00	2.35	0.08	0.19

Appendix 7

Detailed results on the influence of the distribution type

				r = 20 mm	*r* = 30 mm
Size of the lattice					
Maximum lattice size in x =	N/A	mm		40	60
Maximum lattice size in y =	N/A	mm		40	60
Targeted profile					
Thickness =	1	mm			
Second moment of area about x =	N/A	mm4		201093.3	84846.56
Second moment of area about y =	N/A	mm4		201093.3	84846.56
Optimum radius on the lattice in x =	N/A	mm		40	30
Optimum radius on the lattice in y =	N/A	mm		40	30
Optimum area on the lattice =	N/A	mm2		251.327	188.496
Parameters for the first generation of parents					
The initial generation is uniformly or non distributed					
Minimum number of points per parent =	N/A				
Maximum number of points per parent =	N/A				
Number of points per category =	10				
Number of parents per category =	N/A				
Total number of individuals =	N/A				
Total number of individuals in the mating pool =	N/A				
GA parameters					
Maximum number of generations =			100		
Cross-over probability =			0.8		
Mutation probability =			0.01		
Maximum of the individual length to be mutated if mutation occurs =			50	%	
Augmented Lagrangian parameters					
Initial Gamma1 =			2		
Initial Gamma2 =			2		
Initial Mu1 =			0		
Initial Mu2 =			0		
Alpha =			1.5		
Beta =			1.05		

Results

	Run 1			Run 2			Run 3			Run 4			Run 5		
	Area mm2	Ix mm4	Iy mm4	Area mm2	Ix mm4	Iy mm4	Area mm2	Ix mm4	Iy mm4	Area mm2	Ix mm4	Iy mm4	Area mm2	Ix mm4	Iy mm4
r = 20 - Uniform	126.0237	25150.21	25145.65	125.9059	25135.14	25127.1	125.9492	25131.21	25145.81	126.3833	25136.69	25112.17	126.1398	25144.99	25148.37
r = 20 - Non Uniform	125.955	25153.79	25108.69	126.0041	25148.29	25156	126.5242	25152.61	25114.82	126.336	25137.99	25147.77	126.2047	25146.33	25148.46
r = 30 - Uniform	189.7499	84818.73	84845.77	190.2558	84849.55	84863.72	190.9708	84772.68	84942.51	189.4742	84841.03	84787.88	189.9889	84825.34	84877.17
r = 30 - Non Uniform	190.0718	84740.8	84846.13	190.2738	84898.06	84860.09	189.7495	84818.29	84837.01	190.389	84849.13	84851.19	189.367	84892.14	84766.25
	Run 6			Run 7			Run 8			Run 9			Run 10		
	Area mm2	Ix mm4	Iy mm4	Area mm2	Ix mm4	Iy mm4	Area mm2	Ix mm4	Iy mm4	Area mm2	Ix mm4	Iy mm4	Area mm2	Ix mm4	Iy mm4
r = 20 - Uniform	125.9576	25141.15	25143.53	125.8852	25152.6	25132.04	126.3329	25148.91	25167.02	125.9297	25148.29	25148.07	125.8917	25148.91	25149.89
r = 20 - Non Uniform	126.1182	25153.66	25140.47	126.0963	25148.26	25142.24	125.9911	25155.87	25142.59	125.8066	25146.54	25153.95	126.1051	25144.71	25142.58
r = 30 - Uniform	189.9961	84837.67	84903.06	190.1513	84858.77	84852.36	189.6676	84876	84850.56	191.2584	84829.39	84850.53	189.8366	84668.55	84805.91
r = 30 - Non Uniform	190.5777	84780.24	84904.07	190.3753	84869.22	84922.82	189.9258	84698.13	84748.93	189.9024	84824.95	84814.02	189.7794	84812.99	84818.12

Difference relative to optimum

	Run 1			Run 2			Run 3			Run 4			Run 5		
	Area %	Ix %	Iy %	Area %	Ix %	Iy %	Area %	Ix %	Iy %	Area %	Ix %	Iy %	Area %	Ix %	Iy %
r = 20 - Uniform	0.29	0.01	0.01	0.19	0.05	0.08	0.23	0.07	0.01	0.57	0.05	0.14	0.38	0.01	0.00
r = 20 - Non Uniform	0.23	0.02	0.16	0.27	0.00	0.03	0.68	0.02	0.13	0.53	0.04	0.00	0.43	0.01	0.00
r = 30 - Uniform	0.67	0.03	0.00	0.93	0.00	0.02	1.31	0.09	0.11	0.52	0.01	0.07	0.79	0.03	0.04
r = 30 - Non Uniform	0.84	0.12	0.00	0.94	0.06	0.02	0.67	0.03	0.01	1.00	0.00	0.01	0.46	0.05	0.09
	Run 6			Run 7			Run 8			Run 9			Run 10		
	Area %	Ix %	Iy %	Area %	Ix %	Iy %	Area %	Ix %	Iy %	Area %	Ix %	Iy %	Area %	Ix %	Iy %
r = 20 - Uniform	0.23	0.03	0.02	0.18	0.02	0.07	0.53	0.00	0.07	0.21	0.00	0.00	0.18	0.00	0.01
r = 20 - Non Uniform	0.36	0.02	0.03	0.34	0.00	0.02	0.26	0.03	0.02	0.11	0.01	0.02	0.35	0.01	0.02
r = 30 - Uniform	0.80	0.01	0.07	0.88	0.01	0.01	0.62	0.03	0.00	1.47	0.02	0.00	0.71	0.21	0.05
r = 30 - Non Uniform	1.10	0.08	0.07	1.00	0.03	0.09	0.76	0.17	0.12	0.75	0.03	0.04	0.68	0.04	0.03

	Average			Standard deviation			Minimum			Maximum		
	Area %	Ix %	Iy %	Area %	Ix %	Iy %	Area %	Ix %	Iy %	Area %	Ix %	Iy %
r = 20 - Uniform	0.30	0.02	0.04	0.15	0.02	0.05	0.18	0.00	0.00	0.57	0.07	0.14
r = 20 - Non Uniform	0.36	0.02	0.04	0.16	0.01	0.05	0.11	0.00	0.00	0.68	0.04	0.16
r = 30 - Uniform	0.87	0.04	0.04	0.30	0.06	0.04	0.52	0.00	0.00	1.47	0.21	0.11
r = 30 - Non Uniform	0.82	0.06	0.05	0.20	0.05	0.04	0.46	0.00	0.00	1.10	0.17	0.12

Appendix 8

Dimensions and main section properties of a 90 mm wide typical storage rack upright

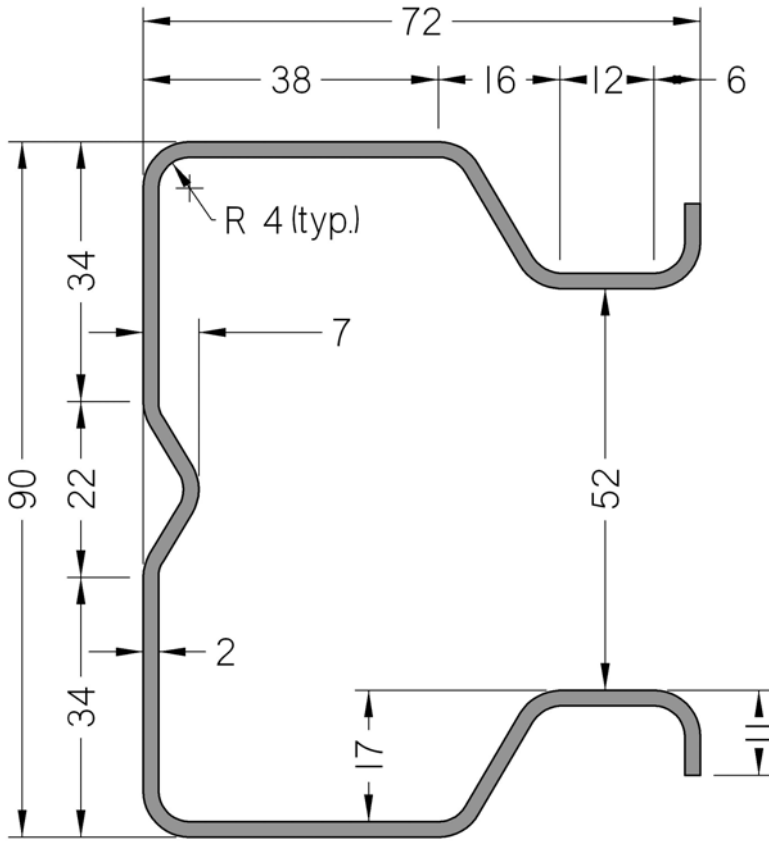

Figure 1: Cross-section dimensions of a typical steel storage rack upright, 90 mm wide, 2 mm thickness

Table 1: Main properties of a typical steel storage rack upright, 90 mm wide, 2 mm thickness

Actual cross-section					Simplified cross-section of 33 elements				
Area (mm^2)	I_x (mm^4)[(1)]	I_y (mm^4)[(1)]	J (mm^4)	Warping (mm^6)	Area (mm^2)	I_x (mm^4)[(1)]	I_y (mm^4)[(1)]	J (mm^4)	Warping(mm^6)
526.3	6.023×10^5	3.232×10^5	701.7	8.249×10^8	515.9	5.922×10^5	3.173×10^5	687.8	7.962×10^8

(1): Second moment of area about the axis of symmetry of the cross-section